

## Response to reviewers

We thank the two reviewers for their constructive comments and helpful suggestions. Below are our responses to each comment.

### Reviewer #1

#### Scientific comments:

##### L26/Introduction:

**The authors should additionally mention the work of Conley et al. (JGR:A 2018, <https://doi.org/10.1002/2017JD027411>) and Kasoar et al. (npj Climate and Atmospheric Science 2018, <https://doi.org/10.1038/s41612-018-0022-z>) which are both highly relevant and could be compared directly with this study. Conley et al. present global temperature changes to removing US SO<sub>2</sub> emissions in three different atmosphere-ocean models, while Kasoar et al. show temperature responses due to re- moving SO<sub>2</sub> emissions individually from either North America, Europe, South Asia, or East Asia in the HadGEM3 atmosphere-ocean model, directly analogous to the present study with NorESM.**

We thank the reviewer for the suggestion. References to Conley et al (2018) and Kasoar et al. (2018) have been added to the manuscript, line 51, 59 and in the Discussion as well as in Summary and Conclusions.

*“...and how these processes are represented in different climate models (Kasoar et al., 2016; Conley et al., 2018).”*

##### L182:

**Are the ‘climatology’ aerosols diagnosed from the control simulation? Or do they come from somewhere else? Essentially, I want to double-check that a free-running control simulation would by construction have zero RF – which might not be the case if the ‘climatology’ isn’t equal to the online control aerosol distribution.**

The climatological aerosols are in this case the native CAM4 aerosols. However, the fixed SST simulations with dual calls were performed for the reference year 2000 aerosol emissions. Thus, the RF is derived from the difference in radiation between two fixed SST simulations: one with year 2000 aerosol emissions and one with the perturbation emissions, and both with meteorology defined by the native CAM4 aerosol. Thus, the RF is by definition zero in the control experiment, to the extent that the atmospheric aerosol loading resulting from the CAM-Oslo aerosol scheme is similar in the fixed SST simulation and the coupled simulation. We agree that the description of the RF simulations is not clear and we have rewritten this sections: line 184-190.

*“The RF is derived from fixed Sea Surface Temperatures (SSTs) simulations where dual calls are made to the radiation code: one call with the CAM4 climatological aerosols and another call where the emission perturbation aerosol concentrations and their effect on cloud albedo are sent to the radiation code solely for diagnosing the radiative effect of these. Thus the meteorology in the RF simulations is identical since the radiative effects of the emission perturbations do not feedback on the meteorology. Similarly, a dual call control simulation with year 2000 aerosol emissions was performed. With this methodology the radiative effects alone from the aerosol can be quantified,*

*without influence of fast or slow feedbacks. The RF simulations are 7 years long and the 5 last years are used for the analysis."*

**Figure 3:**

**Though a nice way of presenting this info, I'm not sure this figure is critical given that some of the information can also be discerned from the error bars e.g. on Fig. 5. The current Fig. 3 could probably be moved to the supplement. Instead, what would be much more useful to include here would be global maps of the temperature changes in each of the experiments, perhaps with shading or stippling to indicate significance at each grid point. This would allow the same comparison as the present Figure 3 in terms of seeing how similar and significant the responses are in different regions, but would also allow for the pattern of the temperature responses to be compared against other studies. I find it odd that this paper does not currently include a single plot which just shows the geographic temperature changes from these experiments, which to me is the first thing I would look at.**

As suggested by the reviewer, Figure 3 has been moved to the supplementary material, and global maps of the temperature response and ERF has been added, also by request from reviewer #2. Please see Figures 5 and 7 in the revised manuscript.

**Table 2:**

**It could be useful to also include the climate sensitivity values (dT/ERF and dT/RF) in this table, as they are used later in the discussion.**

**Table 2: Please include uncertainty ranges**

We agree with the reviewer that it would be useful to include the climate sensitivity values. We have added these values (dT/RF and dT/ERF) to Table 2 as well as standard deviations. Please see Table 2.

**L206/Figure3 plus subsequent figures that have error bars:**

**How is significance determined? The paper frequently discusses whether results from different regions are significantly different from each other, but I am unclear how this was tested for. Similarly error bars are sometimes quoted as one standard deviation, but in the absence of a large ensemble of simulations I'm unclear what it's a standard deviation of.**

The students's t-test is used to determine if the changes are statistically significant. The standard deviations represent the variability of the data from where the mean value is extracted, i.e. from the time series from each simulation. However, in the revised manuscript we have chosen to use the standard error as an uncertainty indication instead of the standard deviation, except for in Table 2. for in Table 2. This information has been added to the manuscript, line 166 -167 and 195-197.

*"All the results presented are annual mean quantities and the first 50 years of each simulations have been removed before averaging and are tested for statistical significance with a student's t-test. Uncertainty ranges for the results are given as standard errors or standard deviations derived from the variability in each simulation."*

**L234:**

Quoting a correlation coefficient for four data points (three of which are pretty much on top of each other) is arguably misleading – it's bound to be close to 1, but this doesn't necessarily tell you much about the strength of the relationship given that not much variation was sampled.

The point is well taken, the correlation has been removed.

**L239-249/Figure 4b:**

This is a very interesting result which I find it hard to get my head around. The whole reason that ERF is widely used is because it has generally been shown to be a better predictor of dT than the instantaneous RF – at least across different and varied forcings. Here you find the opposite – but moreover finding that emission change is an even better predictor of dT! Given that sulfate aerosol has little atmospheric absorption and affects the surface temperatures pretty much entirely through TOA radiative forcing, I would really like to understand why the ERF correlates worse with dT than the emission change. Do the authors have any ideas, physically, how this comes about in these experiments? E.g. maybe some large land-surface responses in the fixed SST experiments, which mean that a substantial portion of the final temperature response is subsumed in rapid adjustments? (N.B. As noted later in the manuscript though, once you include the 0xEU experiment, then ERF does become a better predictor of dT again).

We were also surprised by this result, and we have to admit that we have no definite explanation at this stage. We agree that it would indeed be interesting to better understand why the emission changes predicts the temperature response so well in the emission increase experiments, but a detailed investigation of this is outside the scope of the current study. Our aim with this study is primarily to provide and evaluate coefficients that are easy to use in the context of Integrated Assessment Modelling, and thus we have avoided in depth discussions about the underlying physical mechanisms. Our conjecture at the moment is that this is a manifestation of saturation of aerosol indirect effects which would render the relationship between emission and temperature more linear when emissions continue to increase. This would potentially also explain why RF predicts the global temperature increase well for the emission increase experiments. The result, as the reviewer points out, is only apparent in the experiment where emissions were increased. This is, however, something we would like to study in more detail in the future. This is discussed in the manuscript, line 498-503.

**L262:**

**The SA response can't be weaker in all the latitude bands, or else it would also be weaker globally.**

We thank the reviewer for pointing out this inconsistency in the description of the result. This sentence has been rephrased to clarify that the response in 10xSA is weaker in NHml and ARCT and stronger in SHext and Tropics compared to the other experiments, line 268-270.

*"Thus, the latitudinal temperature responses are in principle indistinguishable for emission increases from EU, NA and EA, while the SA emission response is weaker in NHml and ARCT while it is stronger in SHext and Tropics compared to the other experiments. The spatial distributions of the temperature responses are shown in Figure 5."*

**L263-L270/Figure 6:**

**I'm confused by the different indications of significance. E.g in Figure 6d, the 10xSA ERF in the tropics has an error bar which does not cross zero, and yet it is shaded to indicate that it's not significant. Yet in Fig 6b, the 5xNA ERF in the NHml has a huge error bar that spans zero, but is shaded to indicate that it is significant.**

We have examined the significance for these results looking at the definition of the student's t-test. Here, the fact that the magnitude of the difference between the 5xNA and control simulation is larger than 10xSA and control simulations is the key factor. The absolute difference between the mean values has a larger influence than the difference in the variances in this case for determining if the result is statistically significant. However, the 10xSA result is close to being significant at the 95% confidence level with  $p = 0.065$ .

**L316-318:**

**Consider citing Teng et al. (GRL 2012, doi:10.1029/2012GL051723) which provides a similar example of aerosol forcing over Asia resulting in remote warming over the US, in a different model.**

We thank the reviewer for the reference suggestion. A reference to Teng et al. (2012) has been added, line 543.

*"Moreover, Teng et al. (2012) found a temperature impact in North America directly linked to absorbing aerosols in Asia."*

**L415:**

**Units of climate sensitivity seem to have been inverted here. Check that the number being quoted isn't actually the feedback parameter.**

The number given is indeed a feedback parameter, or climate response parameter, and the value used for the calculations made in the manuscript was the inverted value. The reason for choosing to present the value as a feedback parameter was for transparency with respect to Iversen et al. (2013), Table 1, from where the number is taken. In Iversen et al. (2013), different climate sensitivity estimates are presented as feedback parameters with the units  $Wm^2/K$ . We noticed, however, that the value had inadvertently been miscited and should read 1.101, not 1.01  $Wm^2/K$ . The calculations and figures have been corrected and the conclusions are not affected by this mistake. We have rephrased this paragraph so that it should be clear for the reader that the value cited is the climate sensitivity, line 425.

*"For NorESM this climate sensitivity has been estimated to 0.91  $K/Wm^{-2}$  (Iversen et al., 2013,  $\lambda$  reg in Table 1)."*

**L422:**

**Why is the goal to use model-dependent sensitivities? Surely for integrated assessment modelling, you would like to use a model-independent choice of climate sensitivity? So then, does it matter if you assume a different climate sensitivity and get a different answer (scaled up or scaled down) as a result?**

The point we would like to make in that paragraph is that there is no model-independent sensitivity or RTP coefficient. We see that this was not clear in the manuscript and have rephrased parts of this

paragraph, line 434-439. Even if no climate sensitivity is explicitly applied, there is inherently the climate sensitivity of the model simulations from which the RTP coefficients were derived integrated in the coefficients. The equilibrium sensitivity of the GISS model can only be used by explicitly applying that parameter in the equations for the ARTP. What we wanted to show is how well the RTP coefficients of Shindell and Faluvegi (2010) work without weighting with a climate sensitivity, which means that the sensitivity of that particular model simulation is what is, in effect, used.

If it matters what sensitivity is applied in the equation will depend on what the RTP coefficients will be used for. When comparing the effect of different forcing agents in integrated assessment modelling, it would be crucial, but when comparing the relative latitudinal temperature change distribution, it could be considered less important. However, an assumption about the climate sensitivity always has to be made no matter what the application is, which is what we would like to emphasise. However, an uncertainty related to the RTPs are useful for a sensitivity analysis in the integrated assessment analysis.

**L424:**

**why do you compare with the GISS-E2 transient sensitivity and not equilibrium, given that the NorESM simulations aren't transient?**

The climate sensitivity is an integral part of the formulation of the RTP-coefficients of Shindell and Faluvegi (2010). If a climate sensitivity is not explicitly applied, the implication is that the climate sensitivity from the simulation the RTP coefficients is used. This sensitivity is equal to the transient climate sensitivity of the GISS model (Shindell, 2012). We have rewritten this paragraph to make this clearer for the reader, line 434-439. Please also see discussion above.

*“A third alternative is to apply the RTP coefficients without normalising with a model dependent climate sensitivity parameter, i.e. using the RTP-coefficients of Shindell and Faluvegi (2010), Table 3, directly with forcing estimates (Fig. 14). The implicit assumption in this method is that the sensitivity of NorESM to aerosol forcing is equal to that of the GISS model simulations used to derive the RTP coefficient. This is equivalent with applying the GISS model's sensitivity of 0.5 K/Wm<sup>-2</sup> (Shindell, 2012) in Equation 2. This assumption about the sensitivity leads to RTP-derived temperature responses with smaller RMSD values than both those derived by applying the ECS for NorESM in Equation 1 and 2.”*

**L427-428:**

**I don't agree with this conclusion. The way I read it, using the Shindell and Faluvegi coefficients has reproduced NorESM well here because GISS-E2 has an ECS (i.e. 2 x CO<sub>2</sub>) climate sensitivity of 0.6 K/(Wm<sup>-2</sup>) (Flato et al. IPCC 2013), which happens to be very similar to the sulfate climate sensitivity found for NorESM here. Hansen et al. (JGR 2005, doi:10.1029/2005JD005776) shows that in GISS-E2, the ERF-based sulfate sensitivity is similar to CO<sub>2</sub>. So this doesn't explain why the authors get such different climate sensitivities for sulfate and 2 x CO<sub>2</sub> simulations in NorESM. Maybe due to differences in methodology defining the equilibrium state? Or in calculating ERF (e.g. fixed-SST versus Gregory regression?). At any rate, it would be interesting to understand why NorESM seems to have such a different climate sensitivity for sulfate here compared with the previously published 2 x CO<sub>2</sub> values. The message of e.g. the Hansen et al. (2005) paper is that ERF is a more forcing- independent predictor of temperature change, so it's surprising that the global**

climate sensitivity of NorESM varies so much between forcers. One final point, is that climate sensitivities in general differ hugely between models for the same forcing agent (e.g. the range in Flato et al. is from  $\sim 0.5$  to  $1.5 \text{ K}/(\text{Wm}^{-2})$ ). This is presumably the case for sulfate as much as any other forcer. So, the coincidence that GISS-E2 has a similar climate sensitivity to NorESM doesn't really show that there is smaller variation across models in the sulfate climate sensitivity compared with between different forcers in the same model; this seems quite unlikely to be the case across most models in fact.

The point is well taken, this sentence has been removed. We have also clarified that the climate sensitivity derived from the experiments presented here is not directly comparable to the equilibrium climate sensitivity, line 426-428.

*"This is higher than the sensitivity to aerosol forcing obtained in this study. The climate sensitivity from the simulations presented here is not directly comparable with an equilibrium climate sensitivity, since an equilibrium temperature response would require considerably longer simulations for allowing the ocean to fully adjust."*

#### **L486-487:**

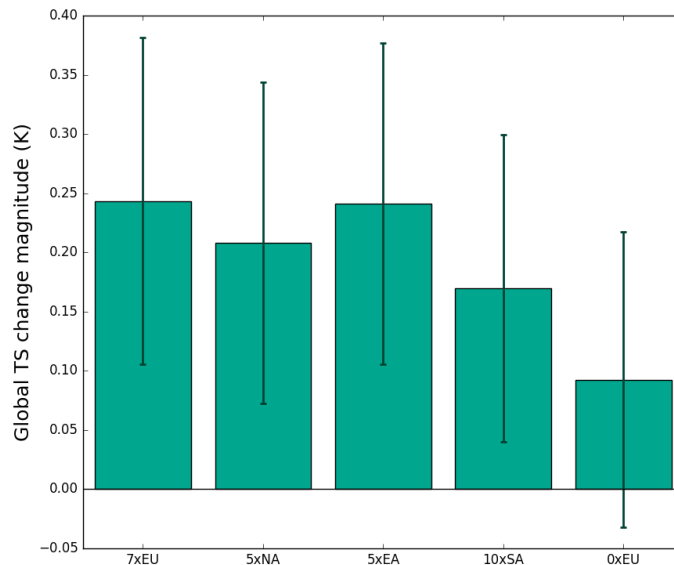
**If saturation of aerosol indirect effects is the explanation here, then shouldn't there be a similar difference in the RF/em as there is in the ERF/em? I don't see how the RF/em can be unaffected by CDNC saturation such that it only shows up as a difference in ERF/em. On a related point: In Figure 4, the error bars for the 0xEU response per em or per RF are enormous and span the entire range of the other experiments. Can the authors be confident that the sensitivity to an emissions reduction actually is any different to an emissions increase, given the considerable overlap of the error bars? It might just be that the smaller forcing and smaller response from the 0x experiment has higher uncertainty because the signal is small compared to internal model variability.**

There is a larger RF response per unit emission for 0xEU compared to 7xEU (Figure 3). In the RF simulations the cloud albedo effect is diagnosed from the cloud distribution determined by the fixed meteorology. Thus, the indirect effect is restricted by the cloud distribution and represent only this first indirect effect (constant cloud water content but changed CDNC). In the ERF simulations the cloud distribution and liquid water content respond to the changed aerosol. In particular, the liquid water path shows large changes which impacts the opacity of the clouds. Thus, including the life-time effect and semidirect effects on clouds amplifies the indirect effects in the ERF simulations compared to the RF simulations.

The results are certainly associated with a lot of uncertainties, as discussed in the manuscript. However, the fact that the results are normalised by the emission change inflates the standard deviation of the 0xEU experiment compared to the other experiments. In fact, the variability is similar in all simulations, see Figure 1 below. The temperature responses in the different experiments have also been tested for significance with the student's t-test, and the global temperature response to European SO<sub>2</sub> emission reductions is found to be statistically different to the temperature responses in emission increase experiments, see Figure S1a. We have now clarified this in the manuscript, line 335-336. We have also emphasised in the text that uncertainties are large and that what we present is no proof of nonlinearity, but an indication that there is no reason to assume that the relationship between emission change and temperature response would be linear, line 561-563.

*“The global average temperature change per unit emission in the emission reduction experiment is significantly different from those in the emission increase experiments (Fig. S1).”*

*“Furthermore, indications were found that the emission-based RTPs derived with NorESM might be non-linear. Removal of anthropogenic European SO<sub>2</sub> emissions led to a temperature response per unit emission approximately twice of that in the 7xEU experiment in NorESM. The result is, however, associated with large uncertainties.”*



**Technical/grammar/typographic comments:**

**L69-70:**

**Confusing wording in this sentence, please re-phrase**

This sentence has been rephrased, line 70-71.

*“Lately, the radiative forcing of long-lived greenhouse gases other than CO<sub>2</sub> have been included in GAINS, which makes it possible to evaluate the changes emissions of these due to air pollution abatement.”*

**L176-177 and Eq3:**

**Inconsistent use of r subscript (emission region or response region?)**

The subscripts have been changed for equation 3 to be consistent with equations 1 and 2.

**L217:**

**add 'typically' or similar caveat**

It has been clarified that this results pertain to the experiments we present in this study, line 224-225.

*“Thus, on a global scale, fast cloud feedbacks contribute to dampen the forcing effect of the emission increases in the NorESM experiments presented here.”*

**Figure 4:**

**The caption should explain how the quantities are normalised. Currently, have to refer to the main text to find out that everything is normalised to the 5xNA experiment in this plot.**

We agree with the reviewer. An explanation has been added to the figure caption of Figure 3.

*“Quantities are normalised by the 5xNA response.”*

**263:**

**Should Figure 6 have been referenced here?**

We thank the reviewer for noticing this mistake. A reference to Figure 6 has been added here, line 272.

**L299:**

**increase -> increases**

The mistake has been corrected, line 307.

**L495: skills -> skill**

We thank the reviewer for noticing. This has been corrected, line 507.

**Reviewer #2**

**Main comments:**

**1) It is worth citing and mentioning Conley et al. (2018), which looks at climate response to removal of US SO<sub>2</sub> emissions. There are some possibilities for comparison and discussion, such as their Table 3 which includes an estimate of temperature response per unit emission change of SO<sub>2</sub>.**

We thank the reviewer for the suggestion. We have now included a citation of Conley et al. (2018) in the manuscript, line 51 and in the Discussion as well as in Summary and Conclusions.

*“...and how these processes are represented in different climate models (Kasoar et al., 2016; Conley et al., 2018).”*



**2) Global maps of the temperature response to each of these SO<sub>2</sub> perturbations would strengthen this paper. Likewise I think global maps of ERF would be interesting as well. This would put the results in context of the few multimodel studies on this topic, such as the one cited above and Kasoar et al. (2016) which you mention already in the manuscript.**

As advised by both reviewer #1 and #2, global maps of the temperature response and the ERF are now added to the manuscript, please see Figure 5 and 7.

**3) The biggest weakness of the paper is the use of a single coupled climate model, especially in a time when multimodel studies are becoming the norm. Ideally, the emissions-based RTP coefficients could be based on an average of several disparate models for more robustness. I understand that it's not feasible to do that in this study, but perhaps the authors could comment on whether or not they expect their results to be robust across additional CMIP models?**

We have added a comparison with the results of Conley et al. (2018) and Kasoar et al. (2018), and we do find similarities between the results. The strong Arctic response is present in these two studies as well, line 533-536.

*"These results are in line with those of Conley et al. (2018), who found a similar latitudinal temperature change distribution in three different models in response to removal of US SO<sub>2</sub> emissions, and Kasoar et al. (2018) who conducted a single model study where they found that the Arctic warmed most in response to removal of SO<sub>2</sub> emissions in different regions."*

**4) In Fig 4a and b, the error bars for just one standard deviation from the mean are quite large for the zero EU SO<sub>2</sub> emissions perturbation. How can the authors then be so sure about a nonlinearity in the response depending on the magnitude and sign of the emissions changes? Since the zero-out EU SO<sub>2</sub> emissions perturbation is much smaller in absolute magnitude than the 7xEU, you would likely need a slightly longer simulation than 160 years to reduce those error bars. Otherwise, I'm not sure how you can rule out the role of internal climate variability.**

Indeed, the 0xEU simulation (and control simulation) is 200 years (line 165). However, the magnitude of the variability is not larger in the 0xEU simulation compared to the other simulations (please also cf. answer to reviewer #1 and Figure 1 above). The non-normalised variability is similar in all simulations. We see that the way of presenting the result as normalised quantities obscures this fact and in the revised manuscript we use the standard error instead of the standard deviation as an indication of uncertainty, line 166-167, and emphasised that the result is associated with uncertainties, line 561-563.

*"Uncertainty ranges for the results are given as standard errors or standard deviations derived from the variability in each simulation."*

*"Furthermore, indications were found that the emission-based RTPs derived with NorESM might be non-linear. Removal of anthropogenic European SO<sub>2</sub> emissions led to a temperature response per unit emission approximately twice of that in the 7xEU experiment in NorESM. The result is, however, associated with large uncertainties."*

**Minor comments**

**1) I'm not really seeing the grey shading in Figure 5? Is it there but just really small?**

The shading colour in what previously was Figure 5, now Figure 4, has been adjusted to appear more grey. Note that it is only the SHext bars in Figure 4 that are shaded grey.

**2) L332-333: this isn't a complete sentence. In general I think the phrase "e.g." is overused in this manuscript and seems to be rather unconventional to start sentences with that abbreviation which happens a couple of times here.**

E.g. has been changed to "For example", line 342. We have gone through the manuscript with particular attention to this phrase and exchanged with equivalent phrase to make the text more varied.

**3) L84: "an comparison" should be "a comparison"**

"An" has been changed to "a", line 86. We thank the reviewer for noticing the mistake.

## References

Conley, A. J., Westervelt, D. M., Lamarque, J. F., Fiore, A. M., Shindell, D., Correa, G., Faluvegi, G., and Horowitz, L. W.: Multimodel Surface Temperature Responses to Removal of US Sulfur Dioxide Emissions, *Journal of Geophysical Research-Atmospheres*, 123, 2773–622 2796, <https://doi.org/10.1002/2017JD027411>, 2018.

Iversen, T., Bentsen, M., Bethke, I., Debernard, J. B., Kirkevag, A., Seland, O., Drange, H., Kristjansson, J. E., Medhaug, I., Sand, M., and Seierstad, I. A.: The Norwegian Earth System Model, NorESM1-M - Part 2: Climate response and scenario projections, *Geoscientific Model Development*, 6, 389–415, <https://doi.org/10.5194/gmd-6-389-2013>, 2013.

Kasoar, M., Shawki, D., and Voulgarakis, A.: Similar spatial patterns of global climate response to aerosols from different regions, *npj Climate and Atmospheric Science*, 1, <https://doi.org/https://doi.org/10.1038/s41612-018-0022-z>, 2018.

Shindell, D. and Faluvegi, G.: The net climate impact of coal-fired power plant emissions, *Atmospheric Chemistry and Physics*, 10, 3247–3260, 2010.

Shindell, D. T.: Evaluation of the absolute regional temperature potential, *Atmospheric Chemistry and Physics*, 12, 7955–7960, <https://doi.org/10.5194/acp-12-7955-2012>, 2012.

Teng, H., Washington, W. M., Branstator, G., Meehl, G. A., and Lamarque, J.-F.: Potential impacts of Asian carbon aerosols on future US warming, *Geophysical Research Letters*, 39, <https://doi.org/10.1029/2012GL051723>, 2012.

# Local and remote temperature response of regional SO<sub>2</sub> emissions

Anna Lewinschal<sup>1,2</sup>, Annica M. L. Ekman<sup>1,2</sup>, Hans-Christen Hansson<sup>2,3</sup>, Maria Sand<sup>4</sup>, Terje K. Berntsen<sup>4,5</sup>, and Joakim Langner<sup>6</sup>

<sup>1</sup>Department of Meteorology, Stockholm University, Stockholm, Sweden

<sup>2</sup>The Bolin Centre for climate research, Stockholm University, Stockholm, Sweden

<sup>3</sup>Department of Environmental Science and Analytical Chemistry, Stockholm University, Stockholm, Sweden

<sup>4</sup>CICERO Center for International Climate and Environmental Research, Oslo, Norway

<sup>5</sup>University of Oslo, Department of Geosciences, Oslo, Norway

<sup>6</sup>Swedish Meteorological and Hydrological Institute, Air Quality Research Unit, Norrköping, Sweden

**Correspondence:** Anna Lewinschal (anna@misu.su.se)

1 **Abstract.** Short-lived anthropogenic climate forcers, such as sulphate aerosols, affect both climate and air quality. Despite  
2 being short-lived, these forcers do not affect temperatures only locally; regions far away from the emission sources are also  
3 affected. Climate metrics are often used e.g. in a policy context to compare the climate impact of different anthropogenic  
4 forcing agents. These metrics typically relate a forcing change in a certain region with a temperature change in another region  
5 and thus often require a separate model to convert emission changes to radiative forcing changes.

6 In this study, we used a coupled Earth System Model (NorESM) to calculate emission-to-temperature-response metrics for  
7 sulphur dioxide (SO<sub>2</sub>) emission changes in four different policy-relevant regions: Europe, North America, East Asia and South  
8 Asia. We first increased the SO<sub>2</sub> emissions in each individual region by an amount giving approximately the same global  
9 average radiative forcing change (-0.45 Wm<sup>-2</sup>). The global mean temperature change per unit sulphur emission compared to  
10 the control experiment was independent of emission region and equal to  $\sim 0.006\text{K/TgSyr}^{-1}$ . On a regional scale, the Arctic  
11 showed the largest temperature response in all experiments. The second largest temperature change occurred in the region of  
12 the imposed emission increase, except when South Asian emissions were changed; in this experiment, the temperature response  
13 was approximately the same in South Asia and East Asia. We also examined the non-linearity of the temperature response by  
14 removing all anthropogenic ~~SO<sub>2</sub>~~ SO<sub>2</sub> emissions over Europe in one experiment. In this case, the temperature response (both  
15 global and regional) was twice of that in the corresponding experiment with a European emission increase. This nonlinearity  
16 in the temperature response is one of many uncertainties associated with the use of simplified climate metrics.

17 *Copyright statement.* TEXT

## 18 1 Introduction

19 Anthropogenic emissions of short-lived climate forcers (SLCFs), i.e. chemical components in the atmosphere that interact  
20 with radiation, have both an immediate effect on local air quality and regional and global effects on the climate in terms of

21 e.g. changes in the temperature and precipitation distribution. Aerosol particles are one of the most important SLCFs due to  
22 their abundance and their effects on health and climate. The short atmospheric residence times of SLCFs such as sulphate  
23 and carbonaceous aerosols (around days) lead to high atmospheric concentrations in emission regions and a highly variable  
24 radiative forcing pattern. Regional radiative forcing can, nevertheless, exert a large influence on the temperature field away  
25 from the forcing region through changes in heat transport or the atmospheric or ocean circulation (Menon et al., 2002; Shindell  
26 et al., 2010; Lewinschal et al., 2013; Acosta Navarro et al., 2016; Dong et al., 2016). Here, we investigate the effect of sulphate  
27 aerosol precursor emission perturbations in different regions on the global surface temperature distribution using a global  
28 climate model.

29 The local radiative forcing by a unit aerosol emission varies from region to region depending on a number of factors,  
30 including e.g. emission location, aerosol processing in the atmosphere and removal rates as well as land surface properties and  
31 cloud distribution (e.g. Bellouin et al., 2016). Moreover, a unit radiative forcing in a specific region may have different impacts  
32 on the temperature response locally in the forcing region and in remote regions away from the forcing, as well as between  
33 different remote regions. In other words, the climate sensitivity in one region can vary depending on the location of the forcing  
34 (e.g. Shindell and Faluvegi, 2009).

35 To facilitate comparisons of the climate effect of different greenhouse gases and emission levels, several climate metrics  
36 have been developed which connect emission changes to radiative forcing, or a specified forcing to a temperature response  
37 (e.g. Aamaas et al., 2013). One appeal of simple climate metrics is that they provide a way to easily evaluate the climate impact  
38 of different air quality or climate mitigation policies without having to run a coupled climate model, something which is not  
39 always feasible due to the computational costs. Because of the even spatial distribution of long lived greenhouse gases, these  
40 metrics have usually described global average quantities. However, the highly variable spatial distribution of aerosol forcing  
41 necessitates the use of metrics that take these spatial inhomogeneities into account (Shine et al., 2005).

42 Shindell and Faluvegi (2009) developed a metric that accounts for spatial inhomogeneities both in the forcing and tempera-  
43 ture response, the Regional Temperature Potential (RTP). With a large set of simulations with one climate model, where they  
44 varied the location of forcing from various anthropogenic climate forcers, these authors derived RTP coefficients that link the  
45 radiative forcing from a climate forcer in a specific region to regional temperature responses. An evaluation of the method for  
46 transient simulations of historical aerosol forcing and response with four different climate models was presented in the work  
47 of Shindell (2012).

48 However, the simplification inherent in the climate metric concept might lead to difficulties related to the generality of these  
49 metrics, such as the RTP. Differences between RTP coefficients derived from different climate models can stem from a number  
50 of different sources, involving everything from atmospheric processing of aerosols, interaction with radiation, aerosol cloud ef-  
51 fects or climate feedbacks, and how these processes are represented in different climate models (~~Kasoar et al., 2016~~) ([Kasoar et al., 2016; C](#)

52 The main objective of this study is to investigate the global and remote impacts of regional sulphate aerosol precursor  
53 emission changes on the surface temperature distribution. This is done by using a coupled atmosphere-ocean model with  
54 interactive aerosol representation, the Norwegian Earth System Model (NorESM). The results from the model simulations are  
55 used to derive RTP coefficients similar to the work of Shindell and Faluvegi (2009). However, our method for deriving RTP

56 coefficients differs from that of Shindell and Faluvegi (2009) in that we derive our RTP coefficients directly from emission  
57 perturbations and focus primarily on the emissions-temperature connection rather than the connection between radiative forcing  
58 and temperature, [similar to Kasoar et al. \(2018\)](#). The RTP coefficients derived by Shindell and Faluvegi (2009) describe the  
59 regional temperature change in response to regional radiative forcing, and essentially describe a regional sensitivity. These  
60 forcing-based sensitivities have to be combined with the radiative forcing patterns derived from emission scenarios with a  
61 chemistry transport model or offline calculations for radiative forcing with a general circulation model to provide the emission-  
62 temperature connection. Another difference is that we focus on emissions from air-pollution and policy-making relevant regions  
63 rather than the latitudinal bands of Shindell and Faluvegi (2009). Thus, we seek to investigate how much an emission change  
64 in one policy relevant region affects both local climate as well as the climate on global scale and in remote regions.

65 The aim is that the RTP coefficients derived with NorESM eventually could be used in Integrated Assessment analysis (IAA),  
66 e.g. such as the Greenhouse gas - Air pollution Interactions and Synergies (GAINS) model. In the GAINS model the climate  
67 impact is estimated using the Global Warming Potential (GWP), which is the global radiative forcing integrated over time  
68 normalised by that of CO<sub>2</sub> (Amann et al., 2011). By the GWP the global climate impact of SLCFs can be taken into account.  
69 Lately, the radiative forcing of long-lived greenhouse ~~gas emission changes due to air pollution abatement, gases~~ other than  
70 CO<sub>2</sub> ~~has been included~~ [have been included in GAINS, which makes it possible to evaluate the changes emissions of these](#)  
71 [due to air pollution abatement](#). Using RTP coefficients in IAA would mean that not only near-term climate effects of changed  
72 SLCF emissions can be evaluated but also how different regions are affected due to specific regional abatement measures. The  
73 RTP can be based on different entities as radiative forcing, effective radiative forcing or direct emissions, which need very  
74 different support calculations respectively. Using the emissions as base for RTPs will provide a very simple way to estimate the  
75 climate impact of changed emissions without having to run a chemical transport model. Using any of the bases for the RTPs  
76 avoids running large coupled climate models. However, the validity of this method relies on the accuracy of the assumption that  
77 the temperature response to changed emissions is linear and that the interaction between different SLCF are negligible for the  
78 resulting temperature response. To address the question regarding linearity in the response depending on emission perturbation  
79 strength we perform simulations with different emission perturbations for the European region.

80 The layout of this study is as follows. First an introduction to the RTP methodology is presented in the method section. The  
81 NorESM model is described together with the experimental design to derive the emission specific RTP coefficients. In Sect.  
82 3 we first present the results from experiments where sulphate aerosol precursor emissions were increased and the global and  
83 regional effect of these emission perturbations. The results of an experiment where European anthropogenic sulphate aerosol  
84 precursor emissions were removed are discussed in the context of non-linearities emerging as a consequence of emission mag-  
85 nitudes. Last in the Result section is ~~an~~ [a](#) comparison of the performance of the forcing-based RTP coefficients of Shindell and  
86 Faluvegi (2009) and Shindell et al. (2012) for NorESM results. The Result section is followed by a discussion and conclusions.

88 **2.1 The Absolute Regional Temperature Potential**

89 There exists a number of different climate metrics that describe the connection between emissions of atmospheric tracer species  
 90 and/or their radiative forcing and/or their effect on the global mean temperature. Many have been developed for the purpose  
 91 of evaluating the impact of increased emissions of long-lived and well-mixed greenhouse gases. Thus, the connection between  
 92 the location of an emission perturbation and the temperature response has not been a primary concern. However, for SLCFs  
 93 the location of the emission perturbation and radiative forcing is a primary matter of interest. A climate metric which takes the  
 94 spatial distribution of these SLCFs and the temperature response into account was developed by Shindell and Faluvegi (2009)  
 95 and Shindell and Faluvegi (2010). The metric describes the temperature change  $dT$  in one area  $a$  at time  $t$ , in response to  
 96 forcing  $F$  in area  $a'$ :

$$dT_a(t) = \int_0^t \left( \sum_{a'} F_{a'}(t') \cdot \frac{dT_a/F_{a'}}{dT_a/F_{global}} \right) \cdot IRF(t-t') dt', \quad (1)$$

97 where the numerator in the second term of the sum,  $dT_a/F_{a'}$ , is the regional response coefficient (cf. Table 3 of Shindell  
 98 and Faluvegi (2010)), which, in this formulation is normalised by the regional temperature response to global average forcing,  
 99  $dT_a/F_{global}$ . The Impulse Response Function,  $IRF$ , represents the time dependent temperature response per unit forcing, i.e.  
 100 the climate sensitivity. For the equilibrium (or quasi-equilibrium or transient) temperature response to a steady forcing, the  
 101  $IRF$  can be replaced by the equilibrium or transient climate sensitivity,  $\lambda$ .

102 Shindell (2012) elaborated the regional temperature change metric of Shindell and Faluvegi (2010) to an Absolute Regional  
 103 Temperature potential,  $ARTP$ , which, in analogue to the Absolute Global Temperature change Potential (AGTP), connects an  
 104 emission perturbation,  $E$ , in region  $r$  of a climate forcer to an absolute temperature change (Shine et al., 2005) in area  $a$ :

$$ARTP_{a,r}(t) = \int_0^t \left( \sum_{a'} \frac{F_{a'}(t')}{E_r} \cdot \frac{dT_a/F_{a'}}{dT_{global}(F_{global})/F_{global}} \right) \cdot IRF(t-t') dt'. \quad (2)$$

105 This formulation uses the global climate sensitivity ( $dT_{global}(F_{global})/F_{global}$ ) to normalise the regional response coeffi-  
 106 cients in contrast to Eq. 1 which uses the regional sensitivity to global forcing. This, i.e. the second term in the summation of  
 107 Eq. 2, yields the unitless RTP coefficients presented in Table 1 of Shindell (2012). Shindell (2012) also advocate the use of the  
 108 latter formulation (Eq. 2) before the former (Eq. 1).

109 The RTP coefficients provided in the work of Shindell and Faluvegi (2010) and Shindell (2012) were derived for forcing in  
 110 four latitude bands covering the globe: the Southern Hemisphere extratropics (90-28°S, SHext), Tropics (28°S-28°N), Northern  
 111 Hemisphere mid latitudes (28-60°N, NHml) and Arctic (60-90°N). These RTP coefficients can be used to estimate the global  
 112 temperature response to any emission perturbation, as long as the forcing in response to the emission perturbation in each of

113 the latitude bands described above is known. The forcing distribution in response to an emission perturbation can be calculated  
114 with e.g. a chemistry transport model (direct radiative forcing only), or with atmospheric general circulation models.

115 In this work, we take our starting point in emission perturbations rather than in the forcing distribution. Sub-global tem-  
116 perature changes in response to emission perturbations are derived both for latitudinal bands following Shindell and Faluvegi  
117 (2009) as well as for the emission regions defined in this study, with the addition of a complementary Arctic region (AR).  
118 This complementary Arctic region is defined as the area north of the Arctic circle ( $66^{\circ}\text{N}$ ), whereas the northernmost latitudinal  
119 band (hereafter denoted ARCT) is defined as the area north of  $60^{\circ}\text{N}$  in accordance with the definition of Shindell and Faluvegi  
120 (2009). All regions that are used in this study are listed in Table 1.

## 121 **2.2 NorESM**

122 The regional temperature changes in response to aerosol emission perturbations are investigated using NorESM (Bentsen  
123 et al., 2013). This model is based on the Community Climate System Model 4.0 (CCSM4.0), but has been modified to include  
124 interactive aerosols and to use the Bergen version of the Miami Isopycnic Coordinate Ocean Model (MICOM) instead of the  
125 Parallel Ocean Program (POP) model. For NorESM the atmospheric component of the model, the Community Atmospheric  
126 Model version 4 (CAM4) has been extended with an interactive aerosol module, CAM4-Oslo (Kirkevåg et al., 2013). The land  
127 surface is represented by the Community Land Model version 4 (CLM4) and sea-ice is modelled with the ice model CICE4.  
128 The atmospheric model uses a finite volume grid with a resolution of  $1.9^{\circ}\times 2.5^{\circ}$  latitude-longitude.

129 The aerosol module in NorESM considers five different aerosol components: sulphate, black carbon, organic matter, mineral  
130 dust and sea salt. Both the mass and number for these aerosol constituents are predicted in a combined sectional and modal  
131 framework. Emissions take place both in the form of primary particles and as precursors to aerosols where the aerosol chemical  
132 compounds are produced through aqueous and gas phase chemical reactions. Aerosols can exist both as external and internal  
133 mixtures, depending on atmospheric processing. E.g. For example, sulphate coating of black carbon, which changes the optical  
134 and hygroscopic properties of this internally mixed aerosol compared with the externally mixed constituents, is accounted for.  
135 Humidification of aerosols is based on the hygroscopicity of the aerosol and the atmospheric relative humidity. Aerosols are  
136 removed from the atmosphere by dry and wet deposition.

137 Aerosol can affect cloud properties through acting as cloud condensation nuclei (CCN). The efficiency of a particular aerosol  
138 depends on its hygroscopicity and size. The amount of aerosol particles that are efficient CCN is connected to the predicted  
139 aerosol size and mass and connected to the two-moment cloud microphysics for stratiform clouds in the model. Thus, NorESM  
140 simulates both the cloud albedo effect and cloud lifetime effects of aerosols. Beside these effects of aerosols on cloud mi-  
141 crophysical properties, semidirect effects which depend on changes of the thermal structure of the atmosphere are accounted  
142 for.

143 An evaluation of the performance of NorESM in simulating the present climate was carried out by Bentsen et al. (2013),  
144 who identified the main biases in the modelled climate compared to observations and that the model simulates a stable climate.  
145 Iversen et al. (2013) derived climate sensitivities for NorESM and investigated the climate response to different future emission

146 scenarios. They found that the CO<sub>2</sub> climate sensitivity of the model is smaller than the Coupled Model Intercomparison Project  
147 phase 5 (CMIP5) multi-model mean, but within one standard deviation.

### 148 2.3 Experiments

149 We perform a suite of model simulations with NorESM where aerosol precursor emissions are perturbed in one region at a  
150 time. Four regions which we consider being of particular interest from an aerosol and air-pollution perspective are studied:  
151 Europe, North America, South Asia and East Asia. The emissions of anthropogenic aerosols have changed considerably in  
152 these regions during the 20th century (e.g. Lamarque et al., 2010).

153 The emission regions (North America - NA, Europe - EU, South Asia - SA and East Asia - EA) are defined according  
154 to the updated region definition of the Task Force on Hemispheric Transport of Air Pollution (HTAP), see Fig. 1, and the  
155 aerosol emissions are the historical emissions of CMIP5 described by Lamarque et al. (2010). The aerosol type we study here  
156 is ammonium sulphates and thus we perturb the anthropogenic sulphur dioxide (SO<sub>2</sub>) emissions provided for CMIP5.

157 Year 2000 is chosen as the baseline year and aerosol emissions, aerosol precursor emissions, trace gas concentrations and  
158 land use representing this year are used for the control simulation. In the emission perturbation experiments, the anthropogenic  
159 aerosol precursor emissions are decreased or increased compared to year 2000 emissions and kept constant in each region  
160 throughout the simulation. In total five coupled sensitivity experiments were performed, four experiments where SO<sub>2</sub> emissions  
161 were increased in the four different regions and one where anthropogenic SO<sub>2</sub> emissions were removed over Europe. The  
162 simulations were started from year 2000 in the transient historical CMIP5 simulation. The simulation length is 160 years  
163 for simulations where emissions are increased. For the experiment where emissions are decreased the simulation length is  
164 200 years. All the results presented are annual mean quantities and the first 50 years of each simulations have been removed  
165 before averaging and are tested for statistical significance with a student's t-test. Uncertainty ranges for the results are given as  
166 standard errors or standard deviations derived from the variability in each simulation.

167 The SO<sub>2</sub> emission changes in the emission perturbation experiments are shown in Fig. 2. In the 0xEU experiment the SO<sub>2</sub>  
168 emissions in Europe are not completely eliminated. There remains 4.66 Tgyr<sup>-1</sup> of volcanic emissions of SO<sub>2</sub> in Europe (from  
169 Etna). The SO<sub>2</sub> emissions in the rest of the experiments were increased by varying amounts depending on the magnitude of  
170 the regional emissions in the control simulation. This was done to obtain a global mean instantaneous radiative forcing of  
171 approximately -0.45 Wm<sup>-2</sup> in all these perturbation experiments. For South Asian emissions, which are low in the control  
172 simulation (6.47 Tgyr<sup>-1</sup> in year 2000 compared with 24.53 Tgyr<sup>-1</sup> in East Asia) the emissions were increased by a factor  
173 of ten. Similarly, for Europe, North America and East Asia, SO<sub>2</sub> emissions were increased by a factor of seven, five and five  
174 respectively.

175 The 0xEU experiment is included so that the effect of emission perturbation magnitude can be investigated, i.e. the sensitivity  
176 to a relatively small emission reduction compared to a relatively large emission increase. The emission perturbation magnitude  
177 (and sign, i.e. reduction) could also be considered as a more likely future scenario.



178 With the resulting global temperature response field of each emission perturbation experiment, RTP coefficients,  $dT_r/dEm_e$  and  $dT_a/dEm_r$ ,  
179 can be constructed relating emission changes in the predefined emission regions,  $er$ , to any response region,  $rg$ , of choice. The  
180 emission-based ARTP can be calculated from the absolute emission change:

$$ARTP_{r,ea,r}^{EM} = \Delta Em_e \frac{dT_r}{dEm_e} \frac{dT_a}{dEm_r}. \quad (3)$$

181 In addition to the coupled experiments we perform simulations to evaluate the Instantaneous Radiative Forcing (RF) and  
182 Effective Radiative Forcing (ERF) of the aerosol emission perturbations in the coupled experiments.

183 The RF is derived from fixed Sea Surface Temperatures (SSTs) simulations where dual calls are made to the radiation  
184 code: one call with [the CAM4 climatological aerosols](#) and another call where the emission perturbation aerosol concentrations  
185 and their effect on cloud albedo are sent to the radiation code solely for diagnosing the radiative effect of these. Thus the  
186 meteorology in the RF simulations is identical since the radiative effects of the emission perturbations do not feedback on the  
187 meteorology. [Similarly, a dual call control simulation with year 2000 aerosol emissions was performed.](#) With this methodology  
188 the radiative effects alone from the aerosol can be quantified, without influence of fast or slow feedbacks. The RF simulations  
189 are 7 years long and the 5 last years are used for the analysis.

190 The ERF is derived by performing fixed SST simulations with aerosol emission perturbations and letting the radiation  
191 changes affect the meteorology. [These simulations are compared to a fixed SST simulation with year 2000 aerosol emissions.](#)  
192 Thus, in addition to the aerosol direct radiative effect and cloud albedo effect the ERF also includes radiative changes from  
193 fast feedbacks such as cloud microphysical and semidirect effects. In NorESM these effects includes e.g. cloud liquid water  
194 content [and](#) cloud fraction. These simulations are 20 years and the 15 last years are used for the analysis. [Similarly to the](#)  
195 [coupled simulations, the RF and ERF are tested for statistical significance with the student's t-test. Standard errors and standard](#)  
196 [deviations from the simulations are used to indicate the uncertainty range.](#)

197 In a simplified manner, the process chain from emission to global mean temperature response can be thought of a translation  
198 of emission to column burden, to the instantaneous direct and indirect radiative forcing, to forcing including fast feedbacks, to  
199 the full coupled temperature response. In an attempt to identify where the largest divergence appears in the process chain from  
200 emission to temperature response in the experiments conducted with NorESM, we investigate the usefulness and accuracy of  
201 alternative quantities to the unit emission in predicting the surface temperature response.

## 202 3 Results

### 203 3.1 Global forcing and temperature response

204 The simplest way to describe the sulphur emission perturbation impact on global and regional temperatures is to express  
205 the temperature response in terms of temperature change per unit emission of sulphur (cf. Sect. 2.1). We first analyse the  
206 results from the sensitivity experiments where SO<sub>2</sub> emissions were increased. The results from the 0xEU experiment will be

207 discussed in Sect. 3.3. The global mean temperature response per unit emission for these sensitivity experiments where the  
208 SO<sub>2</sub> emissions were increased by comparable magnitudes, the global temperature change per unit emission is similar within  
209 10%. The temperature response varies from -0.0056 to -0.0061 K(TgSyr<sup>-1</sup>)<sup>-1</sup>, depending on the location and magnitude of  
210 the sulphur emission change (Table 2).

211 All global mean temperature changes are significantly different compared to the temperature of the year 2000 control sim-  
212 ulation, but are not significantly different between each other (Fig. [S1a in supplementary material](#)). Thus, the location of  
213 an emission change does not appear to be a governing factor for the global mean temperature response modelled by NorESM.  
214 However, all emission changes are located in the northern hemisphere, and atmospheric transport of aerosol particles will con-  
215 tribute to a redistribution of atmospheric concentrations and the resulting column burden and radiative forcing of the aerosol,  
216 so that in some cases the resulting column burden and radiative forcing from emission changes in different regions will partly  
217 overlap.

218 The global average RF per unit emission change (Table 2) shows larger variability than the global temperature response  
219 (varying from -0.010 to -0.017 Wm<sup>-2</sup>(TgSyr<sup>-1</sup>)<sup>-1</sup>, the largest RF value being 62% larger than the smallest value), a larger  
220 emission change is needed in EU than in SA to obtain the same RF change. The variability for the global mean ERF is similar  
221 to that of the RF (difference of 64% between the largest and smallest value, varying from -0.008 to -0.026 Wm<sup>-2</sup>(TgSyr<sup>-1</sup>)<sup>-1</sup>)  
222 but the magnitude of the global mean ERF is smaller than the RF for all emission-increase experiments except for the 5xNA  
223 experiment. Thus, on a global scale, fast cloud feedbacks contribute to dampen the forcing effect of the emission increases in  
224 [NorESM the NorESM experiments presented here](#).

### 225 3.1.1 Emission changes as predictor of global mean temperature change

226 As outlined in Sect. 2, the extreme simplification inherent in the method of describing the temperature response in terms of  
227 emission perturbations, leads to uncertainties related to the generality of the RTP coefficients.

228 Figure 3a illustrates how SO<sub>2</sub> emission perturbations in the different experiments translate to global sulphate column burden,  
229 RF, ERF and temperature anomalies. All values are normalised by the response in the North American experiments to illustrate  
230 the relative amount of variability for each response quantity (i.e. response in the 5xNA experiment is always one in Figure 3.)

231 As noted previously, the global temperature responses per unit emission in the experiments where SO<sub>2</sub> emissions are in-  
232 creased are not significantly different from each other. However, the translation from emission to column burden shows a  
233 different pattern. For this quantity, the column burden per unit emission in the 10xSA experiment is 76% higher than in the  
234 other experiments. Thus, the geographical location seems to be one factor controlling the column burden sensitivity to emis-  
235 sion perturbations in the experiments where emissions are increased. The increased emissions in SA together with a local SA  
236 reduction in precipitation of 0.22 mmday<sup>-1</sup> lead to a longer residence time of sulphate (0.73 days longer) as well as other  
237 aerosol particles in NorESM in the 10xSA experiment compared to the control experiment.

238 A similar pattern as the column burden is evident for the normalised instantaneous RF response to a unit emission change.  
239 The RF response to a unit emission change in SA is larger than the responses in the other experiments. Thus, there appears to  
240 be a close connection between changes in the global sulphate column burden and the RF (correlation coefficient  $r = -0.985$ ). The

241 normalised ERF sensitivity to unit emission perturbations, shows a larger variability between the experiments compared to the  
242 other investigated quantities. The standard deviations for the global average ERF responses are also larger than that for RF.  
243 This result indicates that cloud feedbacks, such as changes in liquid water content or cloud fraction and cloud albedo contribute  
244 substantially to the ERF (cf. Table S1 in supplementary material), and also contributes to larger variability.

245 Figure 3b shows the temperature response normalised by the different "basis quantities" (i.e. the leftmost group of bars in  
246 Fig. 3b are identical to the rightmost bars in Fig. 3a). The perfect basis quantity would be one for which the heights of all  
247 bars corresponding to the different experiments are equal. A basis quantity with this property would be the ideal predictor  
248 of the global mean temperature response. Figure 3b shows that emission perturbation is a good predictor of the temperature  
249 response for emission increases from all regions investigated when emissions are increased in all regions (standard deviations  
250 corresponding the each group of bars are presented in Table 3). Instantaneous RF and column burden as basis quantities  
251 underestimate the temperature response to SA emissions (this is connected to the larger column burden and RF sensitivity  
252 to a unit emission perturbation in SA which do not translate to a larger temperature sensitivity). For ERF there is substantial  
253 variability in the predictability for the temperature responses in the emission increase experiments, which also yields the largest  
254 standard deviation of the basis quantities for these experiments. ~~Thus, emission is a better predictor than the ERF of the global  
255 temperature response for these emission increase experiments.~~

## 256 3.2 Sub-global forcing and temperature response

### 257 3.2.1 Latitudinal forcing and temperature response

258 The sub-global normalised temperature responses in the experiments where SO<sub>2</sub> emissions were increased display more varia-  
259 tion between the different experiments than the global mean sensitivities. (As mentioned before, the 0xEU experiment will be  
260 discussed in Sect. 3.3.2.) The latitudinal temperature responses per unit emission in the experiments with increased emissions  
261 show a qualitatively similar pattern of increasing sensitivity with increasing latitude (Fig. 4). This pattern of Arctic amplifi-  
262 cation is not dependent on the location of the emission perturbation in these experiments, neither in the latitudinal nor the  
263 longitudinal direction. The temperature responses in each latitude band are significantly different from the temperature in the  
264 year 2000 control simulation (at the 99% confidence level), except for the southern hemisphere temperature responses (indi-  
265 cated by gray shading of the columns in Fig. 4). The latitudinal temperature responses in the different experiments are not  
266 significantly different from each other, with the exception of most of the latitudinal temperature responses to SA emissions (at  
267 the 90% confidence level, see Fig. ?? S1 for details). Thus, the latitudinal temperature responses are in principle indistinguish-  
268 able for emission increases from EU, NA and EA, while the SA emission response is ~~generally weaker weaker in NHml and  
269 ARCT while it is stronger in SHext and Tropics compared to the other experiments. The spatial distributions of the temperature  
270 responses are shown in Figure 5.~~

271 The only latitudinal RF and ERF that are statistically significant are the responses to emissions increases in EU, NA and  
272 EA, in NHml, the latitudinal band inside which these emission regions are located (Fig. 6). Significant ERF responses are also  
273 found in ARCT for the same emission source regions, but the ERF is larger in NHml where the emissions changes are located,

274 than in ARCT. SO<sub>2</sub> emissions increases in SA do not lead to any latitudinal average RF or ERF response that are statistically  
275 significant. A large fraction of the atmospheric sulphur mass from SA emissions (which are mainly emitted in the Tropics)  
276 is transported to the NHml region, so that the average RF, ERF and column burden in this region exceeds that of the tropical  
277 region. However, the total integrated sulphur column burden is larger in the Tropics than in the NHml (not shown) in the 10xSA  
278 experiment.

279 The ERF acts to enhance the forcing relative to the RF in the NHml in all experiments, as well as in the ARCT region.  
280 This is a manifestation of aerosol indirect effects which lead to e.g. higher cloud water content (Table S1). The ERF displays  
281 a warming effect in the SHext ([see also Figure 7](#)) in all experiments (due to decreases in low cloud fraction at southern  
282 hemisphere midlatitudes, not shown), although this positive ERF is not significant in any experiment. However, the positive  
283 ERF in the southern hemisphere, which represents a large part of the global mean, contributes to the lower value of global  
284 average of the ERF compared to the RF (cf. Sect. 3.1).

285 As described above, the temperature responses in the latitudinal bands are similar between the experiments with the excep-  
286 tion of the temperature responses to changed SO<sub>2</sub> emissions in SA. SA has the largest tropical response which, however, is only  
287 significantly different from the tropical response to EU emissions, which is the weakest tropical response among the experi-  
288 ments. Similarly, the ARCT response to SA emissions is the smallest among the experiments, and is only significantly different  
289 to the ARCT response to NA emissions, which leads to the strongest response in ARCT. The weaker NHml response to SA  
290 emissions compared to the other emission regions, on the other hand, is significantly different compared to all other NHml  
291 temperature responses. The NA, EU and EA emission regions are to the greater part located in the northern hemisphere mid-  
292 latitudes, and mostly north of the SA emission region. Thus, the longitudinal position of a mid-latitude emission perturbation  
293 does not appear to matter for the latitude mean temperature responses at northern hemisphere high- and mid-latitudes.

### 294 3.2.2 Regional temperature response

295 The differences between the sub-global temperature responses in the different experiments become more evident when they  
296 are derived for the emission perturbation regions (and the AR region north of 66°N) compared to when derived for latitudinal  
297 bands (Fig. 8). All regional temperature changes are statistically significant compared to the control simulation. The largest  
298 temperature response is found in the AR region in all experiments, which is consistent with the latitudinal distribution of  
299 the temperature response for latitude bands described in the previous section. Similarly, the SA emissions have the smallest  
300 effect on the AR temperature among the experiments, but the AR temperature response in this experiment is only significantly  
301 different from the response to NA emissions, which give the largest AR response among the experiments.

302 Outside the AR region, the largest temperature response is found locally in the emission region in all experiments except  
303 10xSA. This result is consistent with the forcing always being largest in the emission region (Fig. 9). The regional RF and  
304 ERF is also statistically significant for local SO<sub>2</sub> emissions from SA, as opposed to when derived for the Tropical latitudinal  
305 band (Fig. 6). For SA emissions the temperature response in the EA region is marginally larger than the local temperature  
306 response in the SA region. The EA region is located downwind of the SA region, which means that a substantial part of the  
307 sulphur emitted in SA is transported to EA and contribute to the local forcing in EA. The column burden ~~increase~~[increases](#)

308 by  $3\%/TgSyr^{-1}$  in EA due to SA emission, to be compared with the increase in EA due to local emission of  $4\%/TgSyr^{-1}$ .  
309 Additionally, advection of air originating from SA might also partly explain the large temperature response in the EA region to  
310 SA emissions. EA is the only region where there are emissions from a remote region (SA) that lead to a temperature response  
311 that is indistinguishable from the effect of local emissions.

312 The local temperature responses in the emission perturbation regions are larger than the corresponding zonal mean temper-  
313 ature responses of the latitudes covered by each region (indicated by black dots in Fig. 8) in all experiments. The largest local  
314 response relative to the zonal mean is found in the 10xSA experiment, which is 66% larger than the zonal mean. The 5xNA  
315 experiment shows the largest absolute difference between the local response and the zonal mean,  $0.0055\text{ K}/TgSyr^{-1}$  (55%  
316 larger). The smallest local temperature response relative the zonal mean is found for 7xEU (20%). All differences between  
317 these local responses and the corresponding zonal means are statistically significant at the 95% confidence level.

318 For both NA and EU emission perturbations, the temperature responses in the regions outside the emission regions are close  
319 to the corresponding zonal mean responses (within 2-17% difference). SA and EA emission perturbations, on the other hand,  
320 both lead to a larger temperature response than the corresponding zonal mean for NA and a smaller temperature response than  
321 the zonal mean for EU, where both these differences between the zonal mean and regional temperature response are statistically  
322 significant. Both EA and SA emission perturbations have a substantial effect on NA temperature, of the same magnitude as the  
323 local responses for these emission regions, despite the geographical distance between the emission location and the temperature  
324 response regions. Local radiative forcing in NA is not responsible for this temperature effect (Fig. 9). This result points towards  
325 a far field effect in the temperature response to Asian aerosol forcing which is mediated by atmospheric circulation changes  
326 rather than radiation changes.

### 327 3.3 Nonlinearities

328 So far, only the results from the experiments where  $SO_2$  emissions were increased have been discussed. In this section we will  
329 focus on the differences between the results from the 0xEU and 7xEU  $SO_2$  emission changes experiments. The purpose is to  
330 investigate if the emission perturbation magnitude or background state influences the temperature response (cf. e.g. Wilcox  
331 et al., 2015).

#### 332 3.3.1 Global temperature response

333 In the experiment where European anthropogenic  $SO_2$  emissions are removed, the global average temperature change per  
334 unit emission is approximately twice of that in the 7xEU experiment, as well as in the other experiments where emissions  
335 were increased (Fig. 3 and Table 2). [The global average temperature change per unit emission in the emission reduction  
336 experiment is significantly different from those in the emission increase experiments \(Fig. S1\)](#). This indicates that there is a  
337 non-linearity depending on the magnitude and sign of the emission change, at least for European  $SO_2$  emissions. Since the  
338 coupled simulations include aerosol indirect effects, and since indirect effects are usually larger than direct aerosol effects  
339 (Rap et al., 2013; Myhre et al., 2013; Kirkevåg et al., 2013), nonlinear effects pertaining to aerosol-cloud interactions most  
340 likely play a role in the difference in global climate sensitivity between the 0xEU and 7xEU experiments. However, effects

341 related to the modeled aerosol microphysics could also play a role in this difference, in particular when SO<sub>2</sub> emissions and  
342 concentrations are low. E.g. For example, in extreme conditions the partitioning between different aerosol microphysical paths  
343 might change, like condensation and nucleation rates of sulphate (Stier et al., 2006).

344 The two experiments with different European SO<sub>2</sub> emission perturbations illustrate the difficulties related to the generality  
345 of the method of translating emission perturbations to temperature response already discussed in Section 3.1. The global mean  
346 temperature responses per unit sulphur emission differ substantially for these two experiments, as well as the magnitudes of  
347 the latitudinal and regional temperature responses.

348 We return to the question of "basis quantities" (cf. Sect. 3.1) and for which step in the translation from emission to tem-  
349 perature response the largest divergence appears for the different experiments. The normalised global temperature responses  
350 per unit emission in the experiments where SO<sub>2</sub> emissions are increased are close to unity, while the normalised temperature  
351 response per unit emission in the 0xEU experiment is larger than two (Fig. 3). The translation from emission to column burden  
352 for the EU emission changes is not dependent on the emission magnitude in the experiments presented here. Similar to what  
353 was noted for the other experiments, the RF per unit emission change in 0xEU and 7xEU is similar to the column burden  
354 response per unit emission change. The normalised ERF sensitivity to unit emission perturbation on the other hand, bears more  
355 resemblance with the temperature response for the 0xEU and 7xEU experiments (third group of bars/the next rightmost bars  
356 in Fig. 3a). This indicates that fast cloud feedbacks, such as cloud lifetime, liquid water content or semidirect effects, is most  
357 likely a key component for understanding the non-linearity in the temperature response to European emissions (cf. Table S1  
358 and S2).

359 Emission perturbation was in Sect. 3.1 found to be a good predictor of the temperature response for emission increases  
360 from all regions investigated when the emissions were increased with similar magnitudes. However, it does not capture the non-  
361 linear behaviour in the temperature response to European emission perturbations of different magnitudes (Fig. 3b). Similarly,  
362 RF and column burden as basis quantities also fail to capture this property in the response to European emission perturbations.  
363 The ERF is the only basis quantity that captures the non-linearity for European emission perturbations of varying magnitude.  
364 However, there is substantial variability in the predictability for the temperature responses in the other experiments. The ERF  
365 shows the smallest standard deviation for the different basis quantities when all experiments are considered (Table 3), but this  
366 is due to substantially larger standard deviations for emissions, CB and RF as basis quantities when the 0xEU experiment is  
367 included. Nevertheless, the ERF is the basis quantity with the highest degree of generality for the global results from all the  
368 experiments conducted with NorESM presented in this study.

### 369 3.3.2 Sub-global temperature response

370 Similarly to the global mean response, the magnitude of the latitudinal and regional temperature responses per unit sulphur  
371 emission are substantially larger in the 0xEU experiment than in the 7xEU experiment, with the exception for the temperature  
372 difference in SA which is not statistically significant compared to the control simulation (Fig. 10, where that hatched bars  
373 indicate the 7xEU response for easy comparison). For the latitudinal sensitivities, the pattern of increasing temperature response  
374 with latitude found in the experiments where emissions were increased (Sect. 3.2.1 and Fig. 4) is also seen for the 0xEU

375 experiment. The relative impact on the southern hemisphere is also larger in this experiment compared to the other experiments.  
376 All latitudinal temperature changes in the 0xEU experiment are significantly different from the responses in all the other  
377 experiments except for the tropical latitude band (Fig. ??S1).

378 The regional 0xEU responses display a similar pattern to the regional responses in the 7xEU experiment, but with different  
379 magnitudes. The largest temperature response is seen in the AR region whereas outside AR the largest response is found in the  
380 emission region (EU). The temperature responses to reduced EU SO<sub>2</sub> emissions in NA and EA are close to the zonal means  
381 for the latitudes covered by these regions (within 2%). This is similar to the the corresponding regional temperature responses  
382 in the 7xEU experiment relative to the zonal mean responses.

383 The non-linear effects are mostly confined to the magnitude of the temperature responses in the case for European emission  
384 perturbations in these experiments. Zonal asymmetries do not appear to have a significant impact on the regional temperature  
385 responses. This might, however, be different for the Asian emission perturbations where zonal asymmetries seem to play a more  
386 prominent role in the regional temperature distributions compared to the European and North American emission perturbations.

### 387 3.4 Comparison with other RTP coefficients

388 In this work we have aimed to establish the simplest possible model for anthropogenic aerosol impacts on regional tempera-  
389 tures, i.e. an emission-based regional temperature potential coefficient.

390 Nevertheless, difficulties associated with nonlinear effects in this relationship remain where ERF proved to be a more general  
391 basis quantity for estimating the global temperature response than emissions, in terms of capturing different magnitudes of  
392 global mean temperature responses for different emission changes in Europe.

393 With the experimental set up applied in this study, it is not possible to derive sub-global (latitudinal or regional) radiative  
394 forcing-based sensitivities, as the forcing changes in the different experiments are not confined to a certain region or  
395 latitude band. However, with the latitudinal and regional RF and ERF from the different experiments, the generality of the  
396 RTP-coefficients derived by Shindell and Faluvegi (2009) and Shindell (2012) can be assessed for the NorESM generated  
397 temperature response. For each experiment the RF and ERF in each latitude band resulting from the regional emission per-  
398 turbations are calculated (Table 4) and used with different methods for calculating the latitudinal temperature responses, the  
399 ARTP.

400 First we compare the temperature response as calculated from Equations 1 and 2 with that from the simulations with NorESM  
401 where SO<sub>2</sub> emissions were increased. Both equations require knowledge of the model global climate sensitivity (or the Impulse  
402 Response Function). The climate sensitivities are derived from the emission perturbation experiments, and we use a mean value  
403 from all experiments with emission increases. Climate sensitivities for both RF and ERF are derived, and these are calculated  
404 to be 0.47 and 0.61 K(Wm<sup>-2</sup>)<sup>-1</sup>, respectively.

405 However, the model global climate sensitivity is not always known, e.g. if the forcing is derived with a Chemistry Trans-  
406 port Model (CTM). Moreover, one motivation behind using RTP coefficients is to avoid conducting multi-century coupled  
407 simulation, which is necessary for deriving the climate sensitivity. Therefore, we also evaluate the performance of the RTP  
408 coefficients with a standardised climate sensitivity as well as applying the RTP coefficients of Shindell and Faluvegi (2010)

409 as regional sensitivity coefficients (i.e. without normalising with the regional climate sensitivity to global forcing and scaling  
410 with the ~~models model's~~ global sensitivity). This is to see how well the RTP-method predicts the model temperature response  
411 when the specific model's climate sensitivity to a particular forcing agent is unknown.

412 The latitudinal temperature responses calculated from Equations 1 and 2 are shown in Fig. 11 and 12. The small dots indicate  
413 the temperature response in specific regions and the filled circles indicate the emission source regions. The high latitude  
414 temperature response in the northern hemisphere (ARCT) calculated using the RTP coefficients, the ARTP, is underestimated  
415 compared to the temperature response in the NorESM experiments (but still within one standard deviation of the NorESM  
416 simulated temperature response), except for when the ERF is used in combination with the normalised coefficients of Shindell  
417 et al. (2012) (Fig. 12b). This is also the method that gives the smallest root mean square deviation (RMSD) of 0.14K (RMSDs  
418 are displayed in each panel). In general, ERF is a better predictor of the latitudinal temperature response than RF, based on  
419 the RMSD. Similarly, the RTP coefficients that are normalised by the global sensitivity (Shindell et al., 2012) rather than the  
420 regional sensitivity (Shindell and Faluvegi, 2010), i.e. Fig. 11 vs. Fig. 12, is a better model for the temperature response in each  
421 latitude band, also based on the RMSD. This was also pointed out by Shindell (2012).

422 However, the performance of this method relies on that the correct climate sensitivity is used and is known. The standard  
423 definition of equilibrium climate sensitivity (ECS) is the equilibrium temperature response to a doubling of CO<sub>2</sub> (Collins et al.,  
424 2013), and is available for nearly all models participating in the Coupled Model Intercomparison Project phase 5 (Flato et al.,  
425 2013). For NorESM this climate sensitivity has been estimated to ~~1.01-0.91 K/Wm<sup>-2</sup> K=1~~ (Iversen et al., 2013) (Iversen et al., 2013,  $\lambda_{reg}$  i  
426 This is higher than the sensitivity to aerosol forcing obtained in this study. The climate sensitivity from the simulations  
427 presented here is not directly comparable with an equilibrium climate sensitivity, since an equilibrium temperature response  
428 would require considerably longer simulations for allowing the ocean to fully adjust. The results of the RTP method with this  
429 ECS applied is shown in Figure 13. Overall, the use of ECS overestimates the temperature response in almost all latitude bands.  
430 Thus, it is important to use ~~the correct climate sensitivity for the climate foreer investigated~~ a climate sensitivity appropriate for  
431 the time scale investigated and possibly also for the particular climate forcer in question. This is a complicating factor since  
432 it requires a priori knowledge of this quantity, which can only be derived by performing coupled simulations, the necessity  
433 of which one often would like to eliminate with a simplified method. Moreover, if calculations to derive radiative forcing are  
434 performed with a CTM, this quantity is not available.

435 A third alternative is to apply the RTP coefficients without normalising with a model dependent climate sensitivity parameter,  
436 i.e. using the RTP-coefficients of Shindell and Faluvegi (2010), Table 3, directly with forcing estimates (Fig. 14). The implicit  
437 assumption in this method is that the sensitivity of NorESM to aerosol forcing is equal to that of the GISS model ~~in Equation  
438 2, a transient simulations used to derive the RTP coefficient. This is is equivalent with applying the GISS model's~~ sensitivity of  
439 0.5 K/Wm<sup>-2</sup> (Shindell, 2012) in Equation 2. This assumption about the sensitivity leads to RTP-derived temperature responses  
440 with smaller RMSD values than both those derived by applying the ECS for NorESM in Equation 1 and 2.

441 ~~Figure 14 shows that assuming that the sulphate aerosol climate sensitivity is similar between different climate models might  
442 be better than assuming that the climate sensitivity for sulphate aerosol is similar to the ECS derived from the same model.~~



444 **4.1 Uncertainties associated with RTP coefficients**

445 The method applied in this work, i.e. evaluating the global and regional temperature responses based on the emission change  
446 magnitudes, means that on the one hand, the starting quantity is easy to assess and compare and is easy to incorporate into  
447 integrated assessment models, such as GAINS. The full response chain from emissions to atmospheric concentrations, to forc-  
448 ing, to surface temperature response is accounted for in this metric. On the other hand, the fact that the metric encompasses  
449 the full chain from emission to temperature response means that there are implicit uncertainties in the metric. The representa-  
450 tiveness of these emission based RTP coefficients will depend on how well the climate model used to derive these coefficients,  
451 represents a large number of atmospheric chemical and physical processes on many different spatial and temporal scales. The  
452 RTP coefficients derived by Shindell and Faluvegi (2009) and Shindell (2012) were derived from radiative forcing, and thus  
453 do not contain the uncertainties introduced when estimating the column burden and forcing associated with aerosol emissions.  
454 However, a model to translate emission to radiative forcing, either RF or ERF, is still necessary to make these forcing based  
455 RTP coefficients useful in an integrated assessment modelling context based on emission pathways.

456 Some major uncertainties can be identified if the emission-temperature response chain is broken down into sub steps. First,  
457 emissions of an atmospheric chemical compound result in an atmospheric concentration and column burden. The translation  
458 from emission of an atmospheric chemical component to atmospheric aerosol loading depends on a number of factors, e.g. if the  
459 aerosol originates from primary emission or is formed through chemical reactions in the atmosphere (i.e. secondary aerosols),  
460 like sulphate which is studied here. The aerosol production for secondary aerosols will depend on which and how chemical  
461 reactions that produce these aerosols are described in the atmospheric model. Kasoar et al. (2016) found that the efficiency of  
462 chemical conversion of SO<sub>2</sub> to sulphate was one process contributing to differences in the simulated responses in three different  
463 climate models to equivalent emission reductions over China. In addition to chemical production, the interaction with clouds  
464 will influence the atmospheric concentration of aerosols. Wet removal through precipitation is an efficient removal process  
465 for hygroscopic aerosols like sulphate containing compounds. All these factors, emission strength, atmospheric production  
466 and removal efficiency influence how long aerosol particles stay in the atmosphere and how far they are transported from the  
467 emission sources. Thus, all these processes influence the atmospheric loading and how these processes are represented in the  
468 model will influence the modelled aerosol column burden.

469 Another source of uncertainty in the emission-forcing-temperature chain, besides the modelled column burden, is how the  
470 aerosol radiative properties are modelled (Myhre et al., 2013). The radiative properties of aerosols depend on e.g. their chemical  
471 composition, water content and mixing state. Thus, given the same atmospheric concentration and distribution of aerosols, their  
472 radiative effect might vary depending on how their radiative properties are represented in the model. Other complicating factors  
473 when it comes to aerosol radiative effects are clouds and aerosol indirect and semi-direct effects on clouds. The direct radiative  
474 forcing will depend on the cloud distribution itself, and aerosol can affect the properties of clouds and also, affect the cloud  
475 distribution, i.e. other components, besides the aerosol itself, within the model influence their radiative effects (Stier et al.,  
476 2013).

477 One of the largest uncertainties associated with the effect of aerosols on climate is related to their indirect effect on clouds  
478 (Myhre et al., 2013) and the representation of these can vary widely between different models. Beside chemical conversion  
479 and radiative impacts, Kasoar et al. (2016) also identified indirect effects on clouds as a major source of diversity between the  
480 models they investigated. Wilcox et al. (2015) found that parameterisations of the relationship between cloud droplet number  
481 concentration and effective radius was the largest contribution to differences in the cloud albedo effect between three models  
482 from the CMIP5 archive, among those NorESM.

483 The factors described above all contribute to inter-model diversity, and will influence how general RTP coefficients are  
484 across models. However, the same processes also contribute to regional sensitivity differences within the same model, but not  
485 based on differences in how the processes are represented in the model, but on the specific meteorological conditions in each  
486 region (e.g. cloud climatology, regional circulation patterns and the background aerosol).

487 ~~It is evident from the~~ The results presented in this study indicate that the temperature sensitivity depends on the emission  
488 change magnitude in NorESM. The global temperature response per unit SO<sub>2</sub> emission in the EU SO<sub>2</sub> removal experiment  
489 is approximately twice of that in the EU SO<sub>2</sub> increase experiment, although the results are also associated with large  
490 uncertainties. The nonlinearity in the response appears to belong to aerosol interactions with clouds and in particular to fast  
491 feedbacks included in the ERF. These include changes in liquid water content, cloud fraction and subsequent changes in cloud  
492 albedo of the new cloud distribution, i.e. cloud life time effects (Albrecht, 1989) (the cloud albedo effect of the background  
493 cloud distribution is included in RF).

494 Wilcox et al. (2015) derived simple functional forms representing the relationship between sulphate load and cloud droplet  
495 effective radius (i.e. the cloud albedo effect) in three different CMIP5 models, with which they could reproduce the time  
496 evolution of the simulated cloud droplet effective radius from historical 20th century simulations. With these functional forms,  
497 they could also quantify the intrinsic varying sensitivity in the parameterisation of the effective radius which depends on the  
498 magnitude of the sulphate load, and how the effective radius (and ultimately radiative forcing) goes from being highly sensitive  
499 at low sulphate loads to a relative insensitive state at high sulphate loads. While they focussed on the cloud albedo effect, the  
500 cloud life time effect is a direct consequence of initial change in effective radius, and should thus display a similar varying  
501 sensitivity depending on the absolute sulphate load.

502 Thus, the similarity of the global temperature responses in the emission increase experiments, despite different mechanisms,  
503 might be due to this saturation of cloud droplet effective radius change when emission increases are large enough. The tem-  
504 perature sensitivity for the different regions could prove to be different if emission were reduced, even by equivalent amounts,  
505 depending on the regional background emission strength and regional meteorological conditions. Nonlinear effects depending  
506 on the emission change magnitude and background is one of the biggest hurdles in creating a general emission based RTP  
507 coefficient.

## 508 4.2 Basis quantity

509 Different quantities for predicting the temperature response have been assessed for the global mean temperature and for latitu-  
510 dinal bands in combination with the RTP coefficients of Shindell and Faluvegi (2010) and Shindell (2012). In both cases ERF  
511 proved to have the best ~~skills~~ skill to predict the temperature response.

512 For the global mean temperature response, the ERF was the only variable that was capable of capturing the large difference  
513 in the temperature responses to the European increase and decrease in SO<sub>2</sub> emissions. However, for the emission increase  
514 experiments, emission ~~was the quantity that best predicted the~~ change was a good predictor for temperature change. Also for  
515 the latitudinal ARTPs the ERF performed better in predicting temperature responses than the RF for NorESM, which is mostly  
516 due to a simulated larger ERF than RF in the Arctic region. This can either be an indication that the sensitivity of the Arctic  
517 region is larger in NorESM than GISS to forcing outside the Arctic region, i.e. that the coefficient relating the forcing to Arctic  
518 temperature responses should be larger for NorESM. It could also be an indication that the cloud feedbacks in the Arctic is a  
519 necessary part of the forcing, and that the local forcing from fast feedbacks is important for the Arctic response in NorESM.

## 520 4.3 Latitudinal and regional sensitivities

521 The sensitivity of zonal mean temperatures to emission perturbations in different regions show large similarities, with the  
522 exception of the overall weaker northern hemisphere temperature response to SA SO<sub>2</sub> emissions; the zonal mean temperature  
523 change increase with increasing latitude in all experiments and do not appear to depend strongly on the location of the emission  
524 perturbations within the northern hemisphere (Fig. 4). There are many factors that might contribute to the weaker temperature  
525 response to the SA emission perturbation. This emission perturbation is located in one of the major monsoonal regions on the  
526 globe, and the increase of sulphate leads to a substantial reduction of precipitation over SA (Table S1 and S2). The reduced  
527 precipitation, in turn, leads to less efficient wet removal of aerosol resulting in an increased residence time and a larger column  
528 burden response per unit emission of both sulphate and BC compared to the control simulation. The decrease in precipitation  
529 in SA (as well as smaller increases in liquid water path, Table S1 and S2) also contribute to a weaker ERF and indirect effect  
530 on clouds, which, in the other experiments enhances the local forcing, but not in SA (Fig. 9). This result is one example of how  
531 different local meteorological conditions where the emission changes occur contribute to different forcing and temperature  
532 responses within the same model.

533 The general pattern, which indicates a stronger temperature response with increasing latitude for all emission perturbations,  
534 is a robust feature in all experiments. In all experiments, the second largest regional sensitivity (after the Arctic region), is  
535 generally found in the region of the emission perturbation. However, for SA emissions, the sensitivity is slightly larger in  
536 the East Asian region compared to the South Asian emission region, a result caused by production of sulphate aerosol from  
537 SO<sub>2</sub> and subsequent transport from SA to EA. These results are in line with those of Conley et al. (2018), who found a  
538 similar latitudinal temperature change distribution in three different models in response to removal of US SO<sub>2</sub> emissions, and  
539 Kasoar et al. (2018) who conducted a single model study where they found that the Arctic warmed most in response to removal  
540 of SO<sub>2</sub> emissions in different regions.

541 Moreover, Asian SO<sub>2</sub> emissions, both from EA and SA, produce larger zonal asymmetries in the global temperature change  
542 field than those of EU and NA. The Asian SO<sub>2</sub> emissions lead to temperature responses in NA and EU that are higher and  
543 lower, respectively, than the zonal mean response. The remote regional temperature responses to EU and NA SO<sub>2</sub> emissions are  
544 on the other hand close to the corresponding zonal mean responses. The location in the Asian monsoon region and proximity  
545 to the Western Pacific mean that these SO<sub>2</sub> emissions could cause tropical precipitation changes that are effective in generating  
546 planetary scale waves. These waves can propagate into the extratropics, which in turn influences the global temperature distri-  
547 bution (Ming et al., 2011; Lewinschal et al., 2013). Moreover, Teng et al. (2012) found a temperature impact in North America  
548 directly linked to absorbing aerosols in Asia.

549 However, the standard deviations for the regional sensitivities are larger than those for the latitudinal sensitivities and zonal  
550 mean sensitivities. Nevertheless, despite the larger uncertainties associated with the regional RTPs compared to the latitudinal  
551 RTPs, they provide information that is not captured by the latitudinal RTPs.

## 552 **5 Summary and Conclusions**

553 We performed simulations with the Earth system model NorESM to evaluate the surface temperature change in response to  
554 SO<sub>2</sub> emission perturbations in Europe, North America and East and South Asia, and to derive emission-based RTP coefficients.  
555 Four experiments were performed where emissions were increased relative to the year 2000 in each individual region to yield  
556 similar global mean radiative forcing values. One additional experiment was performed where anthropogenic SO<sub>2</sub> emissions  
557 were completely removed in Europe.

558 In all five experiments the zonal mean latitudinal temperature change distribution showed a similar pattern of increasing  
559 temperature change with increasing latitude, independently of where the emission perturbation was located. The largest tem-  
560 perature response in all experiments performed was in this study thus found in the Arctic region, no matter where the emission  
561 perturbations were located, similarly to the result of Conley et al. (2018) and Kasoar et al. (2018). Outside the Arctic region,  
562 the temperature response was largest in the emission perturbation region, except for SA emissions where the temperature re-  
563 sponse in the neighbouring EA region was equally large. This result was consistent with the radiative forcing pattern, which  
564 was also strongest in the emission region in each experiment.

565 Furthermore, it was indications were found that the emission-based RTPs derived with NorESM are-might be non-linear.  
566 Removal of anthropogenic European SO<sub>2</sub> emissions led to a temperature response per unit emission approximately twice of  
567 that in the 7xEU experiment in NorESM. The result is, however, associated with large uncertainties. Other differences were also  
568 noticed for the regional responses to regional emission perturbations. Asian emission increases led to a different remote effect  
569 compared to increases in EU and NA emissions. Both EA and SA emission perturbations led to a NA temperature response that  
570 was larger than the zonal mean and an EU response that was smaller than the corresponding zonal mean. EU and NA emission  
571 perturbations, on the other hand, led to remote responses that were close to the zonal mean for the same latitudes.

572 A comparison of the modelled temperature response in NorESM with that calculated using ARTPs (equations 1 and 2)  
573 derived with the RTP coefficients of Shindell and Faluvegi (2010) and Shindell (2012) showed that the RTP coefficients predict

574 similar latitudinal temperature change distributions as those produced by NorESM. The agreement between the calculated  
575 values using ARTPs and the temperature change simulated using NorESM was better when ERF was used together with the  
576 RTP coefficient than when RF was used. This was mainly due to a larger Arctic ERF than RF that resulted in an Arctic  
577 temperature response closer to that produced in the NorESM simulations. This result could be an indication that the Arctic is  
578 more sensitive to forcing outside this region in NorESM than in the GISS model, or that local fast cloud feedbacks are crucial  
579 for the Arctic temperature response in NorESM.

580 Even though the global mean temperature response to emission increases is similar in all regions, the processes leading to  
581 the change may be different in different regions, as it depends on the local meteorological conditions. In all regions except SA,  
582 aerosol indirect effects on clouds, and particularly life time effects, are dominating the ERF response. For SA, direct radiative  
583 effects have a higher relative importance in the response since the local responses in cloud fraction, liquid water path and  
584 precipitation are either weaker compared to the other emission regions or decrease in response to increased SO<sub>2</sub> emissions.  
585 The latitudinal distribution of the zonal mean temperature response to SA emission changes also differs from the rest of the  
586 simulations in that the Northern hemisphere response is weaker and the southern hemisphere and tropical responses are stronger  
587 than in the other simulations.

588 Air pollution globally cause more than 4 million premature deaths each year and as sulphates are major air pollution com-  
589 ponents, emission reductions of SO<sub>2</sub> will be absolutely necessary to improve air quality. The derived emission-based RTPs  
590 will simplify development of cost effective co-beneficial abatement strategies that can give both better air quality and mitigate  
591 climate change. The nonlinear effect predicted by NorESM indicate a reduced immediate climate effect of SO<sub>2</sub> emission re-  
592 ductions in highly polluted areas where the indirect effect is saturated but the effect would become more evident with time as  
593 the saturation of aerosol indirect effects diminishes. Nevertheless, emission reductions of SO<sub>2</sub> and other short-lived climate  
594 forcers are necessary for improving air quality and public health in both Europe, North America and Asia.

595 *Author contributions.* AL, AMLE, HCH, MS, TKB and JL designed the experiments. AL carried out the simulations. AL prepared the  
596 manuscript with contributions from all co-authors.

597 *Competing interests.* The authors declare that they have no conflict of interest.

598 *Acknowledgements.* This work was supported by the Swedish Environmental Protection Agency through the Swedish Clean Air and Climate  
599 research program (SCAC) [and the Research Council of Norway through the EVA \(grant 229771\)](#). The NorESM simulations were performed  
600 on resources provided by the Swedish National Infrastructure for Computing (SNIC) at the National Supercomputer Centre (NSC). [We thank](#)  
601 [two anonymous reviewers for their helpful comments.](#)

## 602 References

- 603 Aamaas, B., Peters, G. P., and Fuglestedt, J. S.: Simple emission metrics for climate impacts, *Earth System Dynamics*, 4, 145–170,  
604 <https://doi.org/10.5194/esd-4-145-2013>, 2013.
- 605 Acosta Navarro, J. C., Varma, V., Riipinen, I., Seland, O., Kirkevåg, A., Struthers, H., Iversen, T., Hansson, H. C., and Ekman, A. M. L.:  
606 Amplification of Arctic warming by past air pollution reductions in Europe, *Nature Geosci.*, 9, <https://doi.org/10.1038/NGEO2673>, 2016.
- 607 Albrecht, B.: Aerosols, cloud microphysics, and fractional cloudiness, *Science*, 245, 1227–1230,  
608 <https://doi.org/10.1126/science.245.4923.1227>, 1989.
- 609 Amann, M., Bertok, I., Borcken-Kleefeld, J., Cofala, J., Heyes, C., Hoeglund-Isaksson, L., Klimont, Z., Nguyen, B., Posch, M., Rafaj, P.,  
610 Sandler, R., Schoepp, W., Wagner, F., and Winiwarter, W.: Cost-effective control of air quality and greenhouse gases in Europe: Modeling  
611 and policy applications, *Environmental Modelling & Software*, 26, 1489–1501, <https://doi.org/10.1016/j.envsoft.2011.07.012>, 2011.
- 612 Bellouin, N., Baker, L., Hodnebrog, O., Olivie, D., Cherian, R., Macintosh, C., Samset, B., Esteve, A., Aamaas, B., Quaas, J., and Myhre, G.:  
613 Regional and seasonal radiative forcing by perturbations to aerosol and ozone precursor emissions, *Atmospheric Chemistry and Physics*,  
614 16, 13 885–13 910, <https://doi.org/10.5194/acp-16-13885-2016>, 2016.
- 615 Bentsen, M., Bethke, I., Debernard, J. B., Iversen, T., Kirkevåg, A., Seland, O., Drange, H., Roelandt, C., Seierstad, I. A., Hoose, C., and  
616 Kristjansson, J. E.: The Norwegian Earth System Model, NorESM1-M - Part 1: Description and basic evaluation of the physical climate,  
617 *Geoscientific Model Development*, 6, 687–720, <https://doi.org/10.5194/gmd-6-687-2013>, 2013.
- 618 Collins, M., Knutti, R., Arblaster, J., Dufresne, J.-L., Fichet, T., Friedlingstein, P., Gao, X., Gutowski, W., Johns, T., Krinner, G., Shongwe,  
619 M., Tebaldi, C., Weaver, A., and Wehner, M.: Long-term Climate Change: Projections, Commitments and Irreversibility., In: *Climate  
620 Change 2013: The Physical Science Basis. Contribution of Working Group I to the Fifth Assessment Report of the Intergovernmental  
621 Panel on Climate Change* [Stocker, T.F., D. Qin, G.-K. Plattner, M. Tignor, S.K. Allen, J. Boschung, A. Nauels, Y. Xia, V. Bex and P.M.  
622 Midgley (eds.)]. Cambridge University Press, Cambridge, United Kingdom and New York, NY, USA., 2013.
- 623 Conley, A. J., Westervelt, D. M., Lamarque, J. F., Fiore, A. M., Shindell, D., Correa, G., Faluvegi, G., and Horowitz, L. W.: Multimodel  
624 Surface Temperature Responses to Removal of US Sulfur Dioxide Emissions, *Journal of Geophysical Reserach-Atmospheres*, 123, 2773–  
625 2796, <https://doi.org/10.1002/2017JD027411>, 2018.
- 626 Dong, B., Sutton, R. T., Highwood, E. J., and Wilcox, L. J.: Preferred response of the East Asian summer monsoon to local and non-local  
627 anthropogenic sulphur dioxide emissions, *Climate Dynamics*, 46, 1733–1751, <https://doi.org/10.1007/s00382-015-2671-5>, 2016.
- 628 Flato, G., Marotzke, J., Abiodun, B., Braconnot, P., Chou, S., Collins, W., Cox, P., Driouech, F., Emori, S., Eyring, V., Forest, C., Gleckler,  
629 P., Guilyardi, E., Jakob, C., Kattsov, V., Reason, C., and Rummukainen, M.: Evaluation of Climate Models., In: *Climate Change 2013:  
630 The Physical Science Basis. Contribution of Working Group I to the Fifth Assess- ment Report of the Intergovernmental Panel on Climate  
631 Change* [Stocker, T.F., D. Qin, G.-K. Plattner, M. Tignor, S.K. Allen, J. Boschung, A. Nauels, Y. Xia, V. Bex and P.M. Midgley (eds.)].  
632 Cambridge University Press, Cambridge, United Kingdom and New York, NY, USA., 2013.
- 633 Iversen, T., Bentsen, M., Bethke, I., Debernard, J. B., Kirkevåg, A., Seland, O., Drange, H., Kristjansson, J. E., Medhaug, I., Sand, M., and  
634 Seierstad, I. A.: The Norwegian Earth System Model, NorESM1-M - Part 2: Climate response and scenario projections, *Geoscientific  
635 Model Development*, 6, 389–415, <https://doi.org/10.5194/gmd-6-389-2013>, 2013.
- 636 Kasoar, M., Voulgarakis, A., Lamarque, J.-F., Shindell, D., Bellouin, N., Collins, W., Faluvegi, G., and Tsigaridis, K.: Regional and global  
637 temperature response to anthropogenic SO<sub>2</sub> emissions from China in three climate models, *Atmospheric Chemistry and Physics*, 16,  
638 9785–9804, <https://doi.org/10.5194/acp-16-9785-2016>, <http://dx.doi.org/10.5194/acp-16-9785-2016>, 2016.

639 Kasoar, M., Shawki, D., and Voulgarakis, A.: Similar spatial patterns of global climate response to aerosols from different regions, *npj*  
640 *Climate and Atmospheric Science*, 1, <https://doi.org/https://doi.org/10.1038/s41612-018-0022-z>, 2018.

641 Kirkevåg, A., Iversen, T., Seland, O., Hoose, C., Kristjánsson, J. E., Struthers, H., Ekman, a. M. L., Ghan, S., Griesfeller, J., Nilsson, E. D.,  
642 and Schulz, M.: Aerosol-climate interactions in the Norwegian Earth System Model - NorESM1-M, *Geoscientific Model Development*,  
643 6, 207–244, <https://doi.org/10.5194/gmd-6-207-2013>, 2013.

644 Lamarque, J.-F., Bond, T. C., Eyring, V., Granier, C., Heil, A., Klimont, Z., Lee, D., Liousse, C., Mieville, A., Owen, B., Schultz, M. G.,  
645 Shindell, D., Smith, S. J., Stehfest, E., Aardenne, J. V., Cooper, O. R., Kainuma, M., Mahowald, N., McConnell, J. R., Naik, V., Riahi,  
646 K., and van Vuuren, D. P.: Historical (1850-2000) gridded anthropogenic and biomass burning emissions of reactive gases and aerosols:  
647 methodology and application, *Atmospheric Chemistry and Physics*, 10, 7017–7039, doi:10.1029/2007GL030541, 2010.

648 Lewinschal, A., Ekman, A. M. L., and Kornich, H.: The role of precipitation in aerosol-induced changes in northern hemisphere wintertime  
649 stationary waves, *Climate Dynamics*, 41, 647–661, <https://doi.org/10.1007/s00382-012-1622-7>, 2013.

650 Menon, S., Hansen, J., Nazarenko, L., and Luo, Y.: Climate effects of black carbon aerosols in China and India, *Science*, 297, 2250–2253,  
651 2002.

652 Ming, Y., Ramaswamy, V., and Chen, G.: A model investigation of aerosol-induced changes in boreal winter extratropical circulation, *Journal*  
653 *of Climate*, 24, 6077–6091, doi: 10.1175/2011JCLI4111.1, 2011.

654 Myhre, G., Shindell, D., Bréon, F.-M., Collins, W., Fuglestedt, J., Huang, J., Koch, D., Lamarque, J.-F., Lee, D., Mendoza, B., Nakajima,  
655 T., Robock, A., Stephens, G., Takemura, T., and Zhang, H.: Anthropogenic and Natural Radiative Forcing., In: *Climate Change 2013:*  
656 *The Physical Science Basis. Contribution of Working Group I to the Fifth Assessment Report of the Intergovernmental Panel on Climate*  
657 *Change* [Stocker, T.F., D. Qin, G.-K. Plattner, M. Tignor, S.K. Allen, J. Boschung, A. Nauels, Y. Xia, V. Bex and P.M. Midgley (eds.)].  
658 Cambridge University Press, Cambridge, United Kingdom and New York, NY, USA, 2013.

659 Myhre, G., Samset, B. H., Schulz, M., Balkanski, Y., Bauer, S., Berntsen, T. K., Bian, H., Bellouin, N., Chin, M., Diehl, T., Easter, R. C.,  
660 Feichter, J., Ghan, S. J., Hauglustaine, D., Iversen, T., Kinne, S., Kirkevåg, A., Lamarque, J. F., Lin, G., Liu, X., Lund, M. T., Luo, G.,  
661 Ma, X., van Noije, T., Penner, J. E., Rasch, P. J., Ruiz, A., Seland, O., Skeie, R. B., Stier, P., Takemura, T., Tsigaridis, K., Wang, P., Wang,  
662 Z., Xu, L., Yu, H., Yu, F., Yoon, J. H., Zhang, K., Zhang, H., and Zhou, C.: Radiative forcing of the direct aerosol effect from AeroCom  
663 Phase II simulations, *Atmospheric Chemistry and Physics*, 13, 1853–1877, <https://doi.org/10.5194/acp-13-1853-2013>, 2013.

664 Rap, A., Scott, C. E., Spracklen, D. V., Bellouin, N., Forster, P. M., Carslaw, K. S., Schmidt, A., and Mann, G.: Natural aerosol direct and  
665 indirect radiative effects, *Geophysical Research Letters*, 40, 3297–3301, <https://doi.org/10.1002/grl.50441>, 2013.

666 Shindell, D. and Faluvegi, G.: Climate response to regional radiative forcing during the twentieth century, *Nature Geoscience*, 2, 294–300,  
667 <https://doi.org/10.1038/NGEO473>, 2009.

668 Shindell, D. and Faluvegi, G.: The net climate impact of coal-fired power plant emissions, *Atmospheric Chemistry and Physics*, 10, 3247–  
669 3260, 2010.

670 Shindell, D., Schulz, M., Ming, Y., Takemura, T., Faluvegi, G., and Ramaswamy, V.: Spatial scales of climate response to inhomogeneous  
671 radiative forcing, *Journal of Geophysical Research-Atmospheres*, 115, <https://doi.org/10.1029/2010JD014108>, 2010.

672 Shindell, D. T.: Evaluation of the absolute regional temperature potential, *Atmospheric Chemistry and Physics*, 12, 7955–7960,  
673 <https://doi.org/10.5194/acp-12-7955-2012>, 2012.

674 Shindell, D. T., Lamarque, J.-F., Schulz, M., Flanner, M., Jiao, C., Chin, M., Young, P., Lee, Y. H., Rotstajn, L., Milly, G., Faluvegi, G.,  
675 Balkanski, Y., Collins, W. J., Conley, A. J., Dalsoren, S., Easter, R., Ghan, S., Horowitz, L., Liu, X., Myhre, G., Nagashima, T., Naik, V.,

676 Rumbold, S., Skeie, R., Sudo, K., Szopa, S., Takemura, T., Voulgarakis, A., and Yoon, J.-H.: Radiative forcing in the ACCMIP historical  
677 and future climate simulations, *Atmospheric Chemistry and Physics*, <https://doi.org/doi:10.5194/acpd-12-21105-2012>, 2012.

678 Shine, K., Berntsen, T., Fuglestedt, J., and Sausen, R.: Scientific issues in the design of metrics for inclusion of oxides of nitrogen in global  
679 climate agreements, *PNAS*, 102, 15 768–15 773, <https://doi.org/10.1073/pnas.0506865102>, 2005.

680 Stier, P., Feichter, J., Kloster, S., Vignati, E., and Wilson, J.: Emission-induced nonlinearities in the global aerosol system: Results from the  
681 ECHAM5-HAM aerosol-climate model, *Journal of Climate*, 19, 3845–3862, <https://doi.org/10.1175/JCLI3772.1>, 2006.

682 Stier, P., Schutgens, N. A. J., Bellouin, N., Bian, H., Boucher, O., Chin, M., Ghan, S., Huneeus, N., Kinne, S., Lin, G., Ma, X., Myhre, G.,  
683 Penner, J. E., Randles, C. A., Samset, B., Schulz, M., Takemura, T., Yu, F., Yu, H., and Zhou, C.: Host model uncertainties in aerosol  
684 radiative forcing estimates: results from the AeroCom Prescribed intercomparison study, *Atmospheric Chemistry and Physics*, 13, 3245–  
685 3270, <https://doi.org/10.5194/acp-13-3245-2013>, 2013.

686 Teng, H., Washington, W. M., Branstator, G., Meehl, G. A., and Lamarque, J.-F.: Potential impacts of Asian carbon aerosols on future US  
687 warming, *Geophysical Research Letters*, 39, <https://doi.org/10.1029/2012GL051723>, 2012.

688 Wilcox, L. J., Highwood, E. J., Booth, B. B. B., and Carslaw, K. S.: Quantifying sources of inter-model diversity in the cloud albedo effect,  
689 *Geophysical Research Letters*, 42, 1568–1575, <https://doi.org/10.1002/2015GL063301>, 2015.



**Table 1.** Latitudinal bands definition and region definitions.

| Name    | Latitudes or region definition |
|---------|--------------------------------|
| SHext   | 90°S-28°S                      |
| Tropics | 28°S-28°N                      |
| NHml    | 28°N-60°N                      |
| ARCT    | 60°N-90°N                      |
| AR      | 66°N-90°N                      |
| EU      | Europe - HTAPv2                |
| NA      | North America - HTAPv2         |
| EA      | East Asia - HTAPv2             |
| SA      | South Asia - HTAPv2            |

**Table 2.** Global results from the experiment where SO<sub>2</sub> emissions in different regions are changed. Units are 10<sup>-2</sup>K/TgSyr<sup>-1</sup> for temperature ~~and change per emission change~~, 10<sup>-2</sup>Wm<sup>-2</sup>/TgSyr<sup>-1</sup> for RF and ERF ~~per emission change and K/Wm<sup>-2</sup> for temperature change per unit RF and ERF~~. Standard deviations are in parentheses.

| Experiment           | 0xEU SO <sub>2</sub> | 7xEU SO <sub>2</sub> | 5xNA SO <sub>2</sub> | 5xEA SO <sub>2</sub> | 10xSA SO <sub>2</sub> |
|----------------------|----------------------|----------------------|----------------------|----------------------|-----------------------|
| $\Delta T/\Delta em$ | -1.28(1.72)          | -0.56(0.32)          | -0.61(0.40)          | -0.58(0.29)          | -0.58(0.45)           |
| RF/ $\Delta em$      | -1.30(0.02)          | -1.04(0.02)          | -1.22(0.04)          | -1.14(0.04)          | -1.68(0.01)           |
| ERF/ $\Delta em$     | -2.55(0.04)          | -0.78(0.75)          | -1.29(1.03)          | -1.00(0.87)          | -0.88(1.08)           |
| $\Delta T/RF$        | 0.99(1.33)           | 0.54(0.31)           | 0.50(0.32)           | 0.51(0.26)           | 0.35(0.27)            |
| $\Delta T/ERF$       | 0.50(1.27)           | 0.72(0.67)           | 0.47(0.46)           | 0.58(0.54)           | 0.66(0.87)            |

**Table 3.** Standard deviations for the different normalised basis quantities evaluated in Figure 3b (unitless).

| Variable            | EM   | HRF-RF | ERF  | CB   |
|---------------------|------|--------|------|------|
| Increased emissions | 0.03 | 0.15   | 0.19 | 0.17 |
| All experiments     | 0.46 | 0.43   | 0.19 | 0.51 |

**Table 4.** Regional radiative forcing (RF) and effective radiative forcing (ERF) in  $\text{Wm}^{-2}$  used to derive latitudinal ARTPs in Fig. 11-14.

| Experiment | 0xEU SO <sub>2</sub> | 7xEU SO <sub>2</sub> | 5xNA SO <sub>2</sub> | 5xEA SO <sub>2</sub> | 10xSA SO <sub>2</sub> |
|------------|----------------------|----------------------|----------------------|----------------------|-----------------------|
| RF         |                      |                      |                      |                      |                       |
| SH         | 0.000                | -0.003               | -0.003               | -0.024               | -0.038                |
| TROP       | 0.037                | -0.239               | -0.224               | -0.388               | -0.685                |
| NHml       | 0.329                | -1.423               | -1.415               | -1.315               | -0.729                |
| ARCT       | 0.171                | -0.859               | -0.488               | -0.413               | -0.143                |
| ERF        |                      |                      |                      |                      |                       |
| SH         | 0.729                | 0.608                | 0.663                | 0.511                | 0.628                 |
| TROP       | 0.081                | -0.170               | -0.415               | -0.330               | -0.489                |
| NHml       | -0.184               | -1.774               | -1.710               | -1.752               | -0.904                |
| ARCT       | -0.139               | -1.046               | -0.900               | -1.075               | -0.149                |

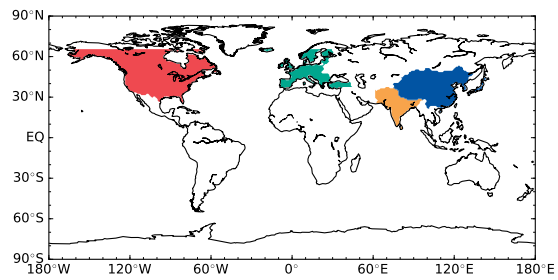


**Figure 1.** Emission regions according to the HTAP definition. The colours represent: green - Europe (EU), red - North America (NA), blue - East Asia (EA) and yellow - South Asia (SA).

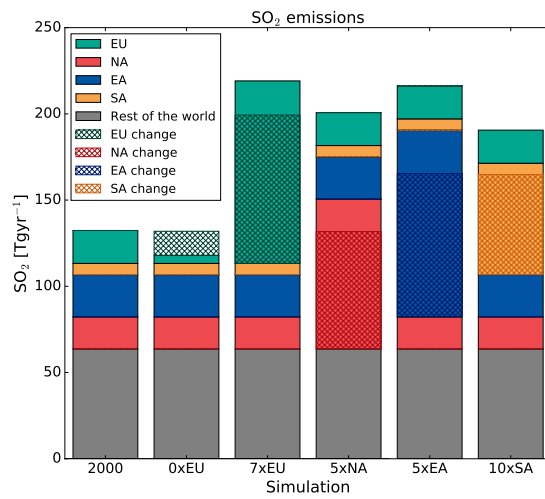


**Figure 2.** Global annual SO<sub>2</sub> and regional emissions and emission differences in the simulations. Each column shows the total global SO<sub>2</sub> emissions in each simulation and the colour shading indicates the contribution from each region. Hatching indicates the emission change relative to the year 2000 simulation.

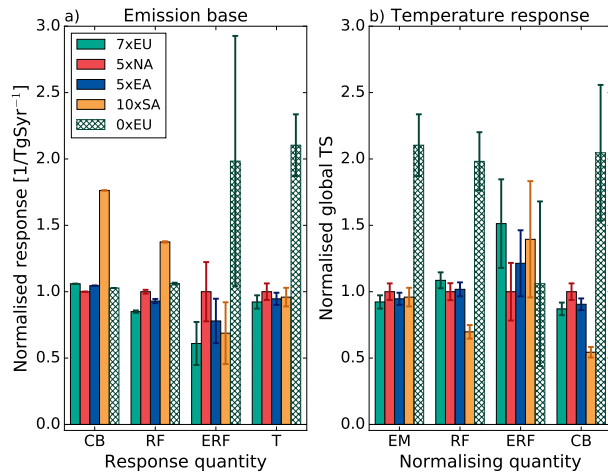


**Figure 3.** Normalised a) column burden (CB), radiative forcing (RF), effective radiative forcing (ERF) and temperature (T) per unit SO<sub>2</sub> emission, and b) normalised temperature response per emissions, RF, ERF and CB in the different experiments. Quantities are normalised by the 5xNA response. The error indicate bars show one the standard deviation error.

690 Significance levels for temperature differences between the different experiments, for the temperature response regions a)  
 691 global mean, b) SHext, c) Tropics, d) NHml, e) ARCT, f) EU, g) NA, h) EA, i) SA and j) AR.

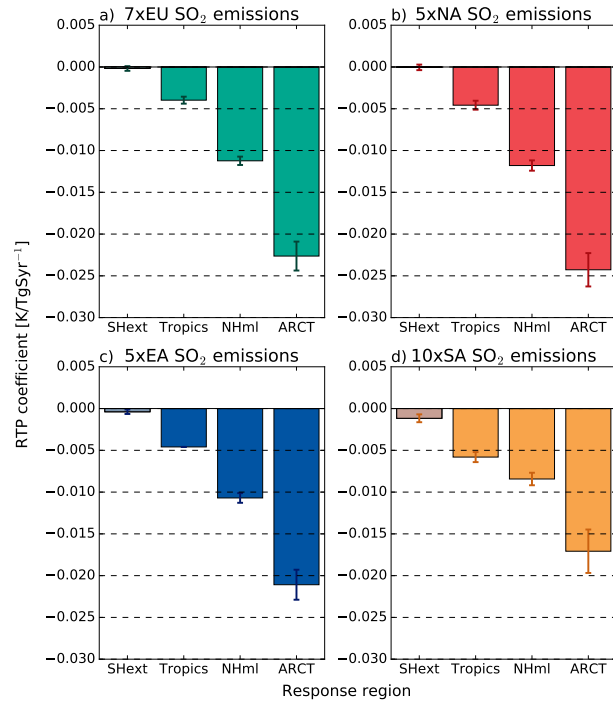


**Figure 4.** Latitudinal RTP coefficients for SO<sub>2</sub> emission [K/TgSyr<sup>-1</sup>] for a) EU emissions b) NA emissions c) EA emissions and d) SA emissions. Grey shading indicates that the temperature change is not statistically significant ( $p > 0.05$ ) compared to the control simulation. The error bars indicate one show the standard deviation error.



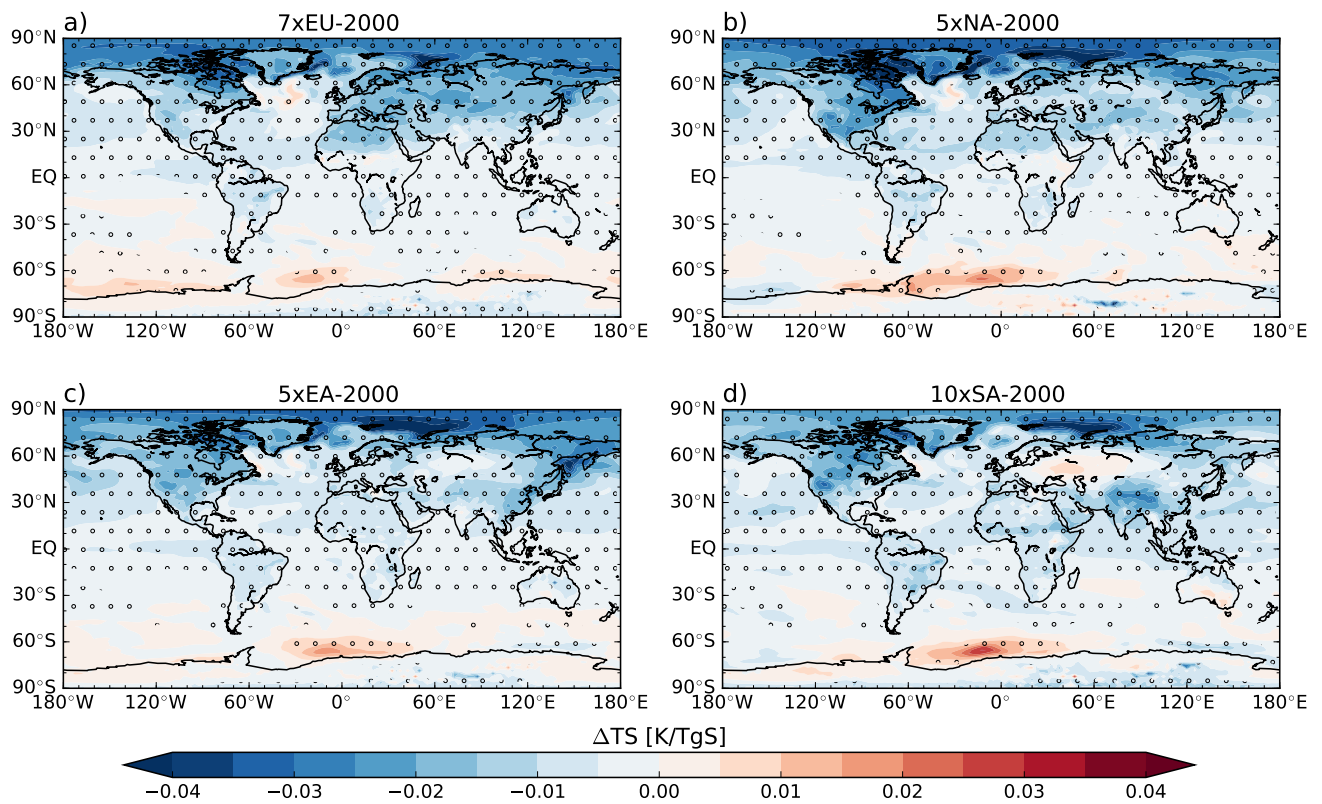


**Figure 5.** Global temperature change per unit SO<sub>2</sub> emission for a) 7xEU, b) 5xNA, c) 5xEA, d) 10xSA compared to the control simulation. Dots indicate where the result is statistically significant at the 95% confidence level.

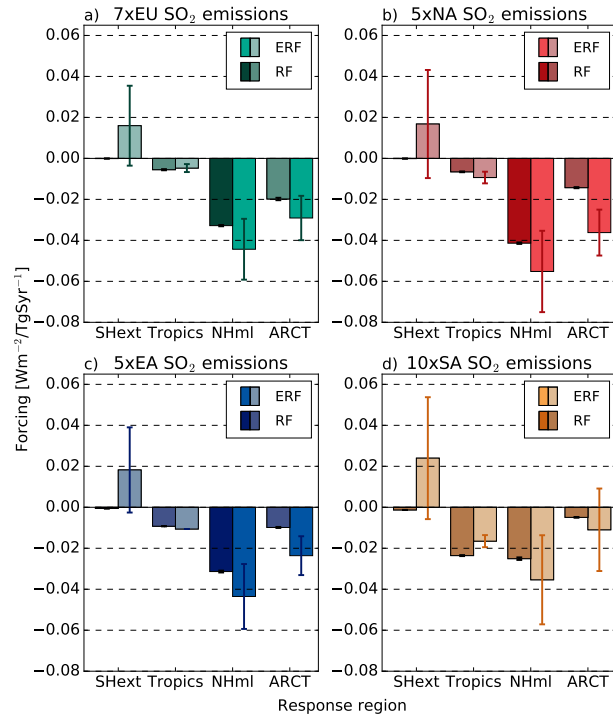


**Figure 6.** Latitudinal RF and ERF for  $\text{SO}_2$  emission [ $\text{Wm}^{-2}/\text{TgSyr}^{-1}$ ] for a) EU emissions b) NA emissions c) EA emissions and d) SA emissions. In each pair of bars the left bar indicated RF and the right bar indicated ERF. Grey shading indicates that the forcing response is not statistically significant ( $p > 0.05$ ) compared to the control simulation. [The error bars show the standard error.](#)

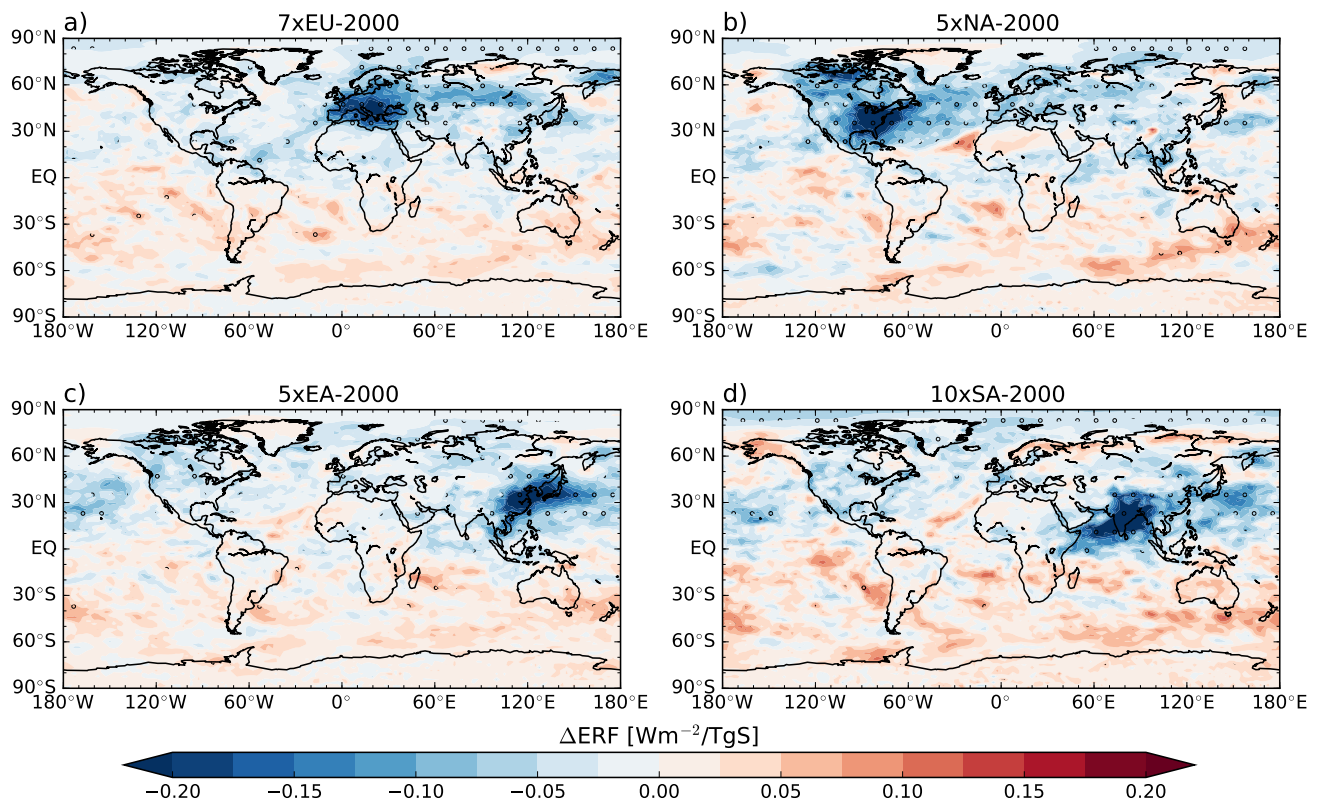


**Figure 7.** Global effective radiative forcing per unit  $\text{SO}_2$  emission for a) 7xEU, b) 5xNA, c) 5xEA, d) 10xSA compared to the control simulation. Dots indicate where the result is statistically significant at the 95% confidence level.

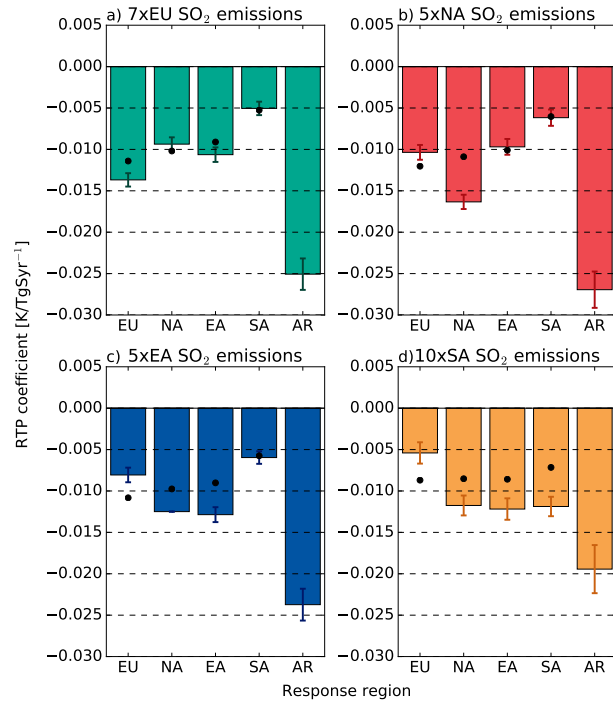


**Figure 8.** Regional RTP coefficients for SO<sub>2</sub> emission [K/TgSyr<sup>-1</sup>] for a) EU emissions b) NA emissions c) EA emissions and d) SA emissions. Grey shading indicates that the temperature change is not statistically significant ( $p > 0.05$ ) compared to the control simulation. The error bars indicate one show the standard deviation error. Black dots indicate the zonal mean for the latitudes that cover each region.

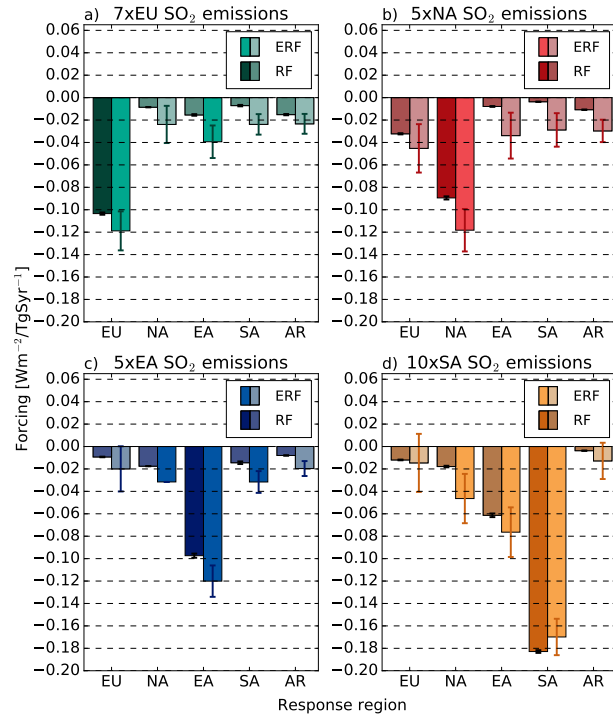


**Figure 9.** Regional RF and ERF for SO<sub>2</sub> emission [Wm<sup>-2</sup>/TgSyr<sup>-1</sup>] for a) EU emissions b) NA emissions c) EA emissions and d) SA emissions. In each pair of bars the left bar indicated RF and the right bar indicated ERF. Grey shading indicates that the forcing response is not statistically significant ( $p > 0.05$ ) compared to the control simulation. The black dots indicate the zonal mean of error bars show the latitudes covering each response region standard error.

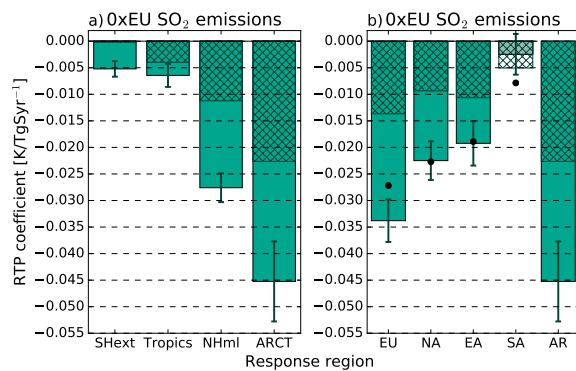


**Figure 10.** Latitudinal (a) and regional (b) RTP coefficients for 0xEU SO<sub>2</sub> emissions. [K/TgSyr<sup>-1</sup>]. Grey shading indicates non-statistical differences ( $p > 0.05$ ). The hatching indicated the RTP for 7xEU emissions (cf. Fig. 4 and 8) for easy comparison. [The error bars show the standard error.](#)

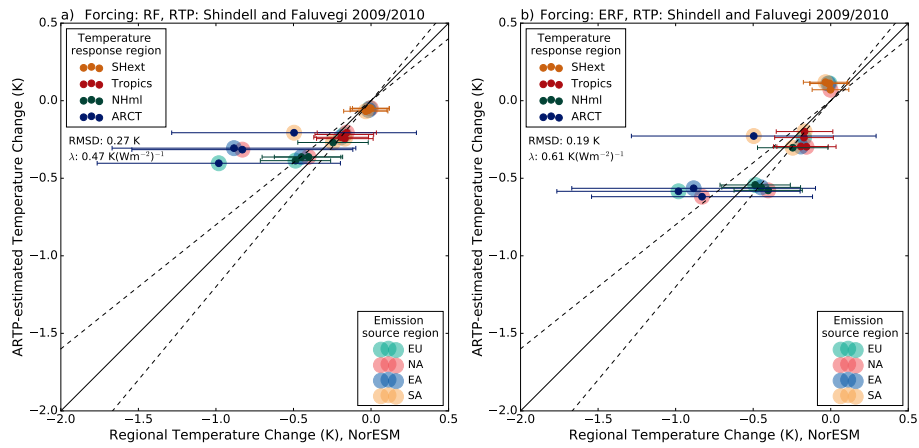


**Figure 11.** Regional temperature change from the coupled simulations (horizontal axis) compared with the estimated temperature response when using a) RF and b) ERF in combination with the RTP coefficients of Shindell and Faluvegi (2009), Eq. 1 with the climate sensitivity derived from the current experiments (vertical axis). The horizontal bars indicate one standard deviation for the temperature response in the coupled simulations. The dashed lines show  $\pm 20\%$  agreement threshold.

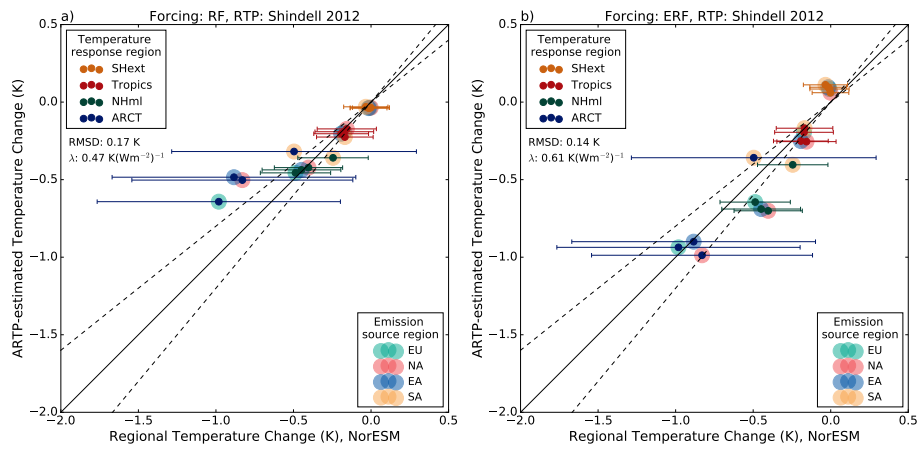


**Figure 12.** As Fig. 11 but with the RTP coefficients of Shindell (2012), Eq. 2 with the climate sensitivity derived from the current experiments.



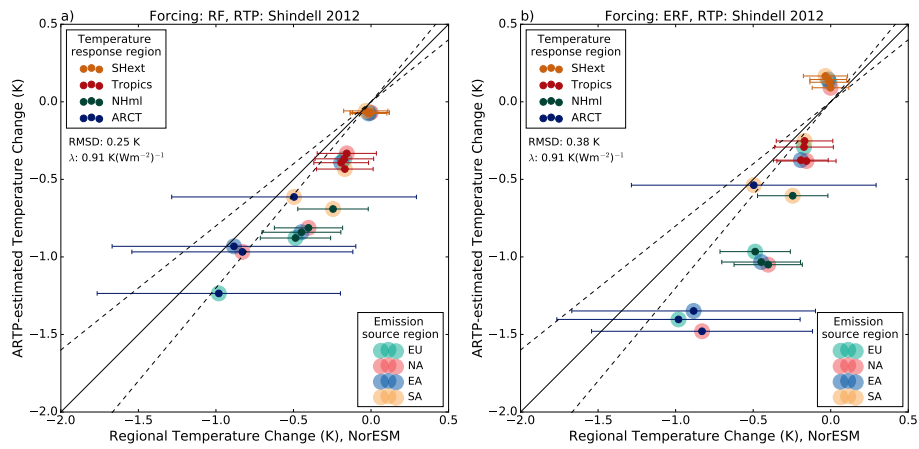


**Figure 13.** As Fig. 11 but with the RTP coefficients of Shindell (2012), Eq. 2 with the  $\text{CO}_2$  sensitivity from Iversen et al. (2013).

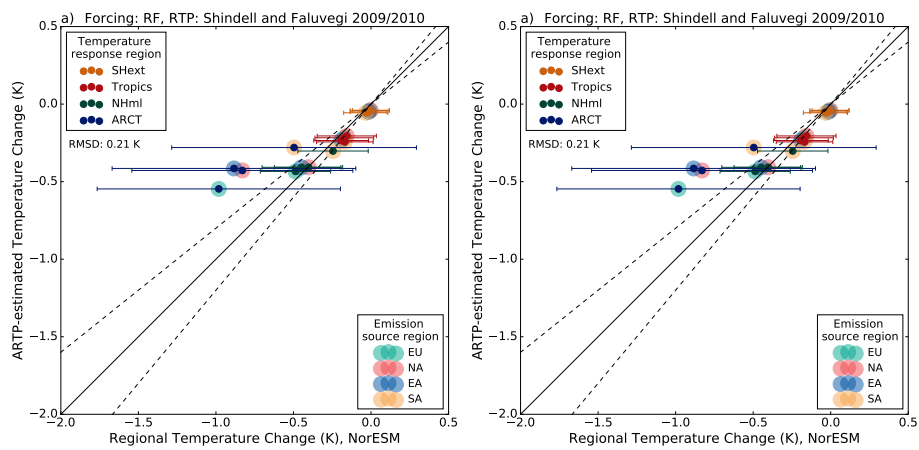


**Figure 14.** As Fig. 11 but with the RTP coefficients of Shindell and Faluvegi (2009), and with no climate sensitivity applied.